

Review

# Ecological and Wildfire Responses to Rapid Landscape Changes within the Last ~900 Years on the South Haven Peninsula, Dorset (Southern England)

Daniel Howlett, Sabine Wulf \*, Scarlett Wharram, Mark Hardiman and Harry Byrne

School of the Environment, Geography and Geosciences, University of Portsmouth, Buckingham Building, Lion Terrace, Portsmouth PO1 3HE, UK; dan.howlett29@gmail.com (D.H.); srwharram@gmail.com (S.W.); mark.hardiman@port.ac.uk (M.H.); harrymorganbyrne@gmail.com (H.B.)

\* Correspondence: sabine.wulf@port.ac.uk

**Abstract:** A multi-proxy palaeoenvironmental dataset (LOI, pollen, charcoal, grain sizes and the humification index) was extracted and radiocarbon dated from a sedimentary sequence from Spur Bog, central South Haven Peninsula (Dorset, southern England) to reconstruct ecological and environmental changes within the last ~900 years. These analyses reveal highly unstable environmental conditions at the site, evidencing the occurrence of multiple, often rapid changes during this period. The results significantly expand upon the existing palaeoenvironmental and geomorphological frameworks of the South Haven Peninsula which previously relied upon sparse, vague historical records prior to ~1750 AD. The multi-proxy dataset of Spur Bog sediments recorded a primary “development” phase (~1150–1470 AD) during which marine processes were the dominant control upon environmental conditions at the site, resulting in marked geomorphological changes that lead to the progressive eastward expansion of the South Haven Peninsula. This is followed by a secondary “maturation” phase (~1470–1880 AD) during which the Spur Bog sequence exhibits significant ecological changes in response to fluctuations in sea level, coastal erosion and human activity, demonstrating the vulnerability of the site to future climatic and anthropogenic pressures.

**Keywords:** ecology; wildfire; landscape changes; Spur Bog; South Haven Peninsula; southern England; late Holocene



**Citation:** Howlett, D.; Wulf, S.; Wharram, S.; Hardiman, M.; Byrne, H. Ecological and Wildfire Responses to Rapid Landscape Changes within the Last ~900 Years on the South Haven Peninsula, Dorset (Southern England). *Quaternary* **2022**, *5*, 27. <https://doi.org/10.3390/quat5020027>

Academic Editor: Juan Manuel López García

Received: 11 February 2022

Accepted: 28 April 2022

Published: 4 May 2022

**Publisher's Note:** MDPI stays neutral with regard to jurisdictional claims in published maps and institutional affiliations.



**Copyright:** © 2022 by the authors. Licensee MDPI, Basel, Switzerland. This article is an open access article distributed under the terms and conditions of the Creative Commons Attribution (CC BY) license (<https://creativecommons.org/licenses/by/4.0/>).

## 1. Introduction

Due to their sensitivity to rapid geomorphological and ecological changes [1,2], coastal environments are acutely vulnerable to the impacts of anthropogenic pressures and future climate uncertainty, such as sea level rise, coastal flooding and groundwater salinisation [3]. In addition, coastal environments are of significant socio-economic-ecological importance, presenting significant risks to environmental processes and human activities should these areas become destabilised [4,5]. The South Haven Peninsula, Dorset (southern-central England), supports numerous internationally important habitats, including *Spartina* salt marshes, sand dunes, wetlands, peat bogs and heathlands, resulting in substantial research focus upon the area [6–10]. Historical records reaching back to the late 16th century AD indicate rapid geomorphological changes in this area which were most likely accompanied by significant environmental changes, although the exact timings and driving mechanisms of which are currently uncertain.

Today, much of the South Haven Peninsula is a National Reserve and forms part of the Dorset Area of Outstanding Natural Beauty, which, due to its rich biodiversity, attracts millions of visitors each year. In response to the rapid geomorphological changes at the Peninsula and in light of current climate change, i.e., rising sea level and increasing storm frequency, a ‘Shifting Shores’ coastal change policy was launched by National Trust in 2005 in order to aid the recognition and planning of coastal properties in the Purbeck/Studland

area, to ensure that continuing tourism does not impede upon the conservation of natural habitats [11]. One active management strategy is controlled burning to preserve heathland habitats near the study site [11].

The aim of this study is to provide quantitative evidence and a timeline for past geomorphological and ecological changes in response to rapid climate and environmental change by applying a multi-proxy approach (pollen, charcoal, humification, and grain sizes) on a sediment core from Spur Bog located on the south-central part of South Haven Peninsula. These results are critical for better understanding and facilitating the effective mitigation of the risks by the National Trust associated with future climate uncertainty and anthropogenic pressures in these regions.

## 2. Study Site

### 2.1. Location of Spur Bog and Geology of South Haven Peninsula

Spur Bog is an area of wetland situated on the south-western shore of the coastal freshwater lake 'Little Sea' on the South Haven Peninsula in Dorset, southern England (Figure 1). The site is located within the Studland and Godlingston Heath National Nature Reserve (SSSI) and managed by the National Trust. Presently, environmental conditions at the Spur Bog are that of an ombrotrophic lowland bog supporting wet acidophilus heath and shrubs. The Spur Bog is constrained by an area of *Betula*- and *Pinus*-dominated woodland to the south referred to as 'Twelve Acre Wood', whilst dry heathland of Spur Heath, the Little Sea and Ferry Road constrain the Spur Bog to the north, east and west, respectively.

The geology of the South Haven Peninsula is characterised by Palaeocene sedimentary rocks in the western part, specifically by the Broadstone Clays and overlying Parkstone Clays and Sands of the Eocene Poole Formation (formerly 'Bagshot Beds'), which are locally overlain by Pleistocene fluvial terraces [12–14]. The geology of the central and eastern part of the Peninsula is entirely made up of young (>400 years) dune ridges (aeolian sand), beach sands and gravel deposits (Figure 1d).

The cliffs of the Poole Formation east of Bournemouth and in the south of Studland Bay (Figure 1c) are the main sources of material that have continuously supplied the accumulation of sand and gravel along the mostly wind-protected eastern shore of the South Haven Peninsula over the last >400 years [14,15]. Figure 1c (see below) depicts the main sediment transport processes within the Studland Bay area. The original coastline was located at the western shore of Little Sea, which is today marked by 6–9 m rises in elevation onto the Plateau Heath (Figure 1d) [14]. Though most of the South Haven Peninsula is sheltered from prevailing south-westerly winds and storms, some considerable erosion occurs at the southern shores of Studland Bay and at the northern end of the Peninsula (Figure 1c). Eroded sediments from the south are transported northwards along the shoreline (littoral drift that aligns with prevailing winds; yellow arrow in Figure 1c) and deposited in the north-eastern part of South Haven Peninsula, predominantly forming the long-term extension of the spit [11,16]. Seasonal weather fluctuations can furthermore initiate wave-driven sediments to be pushed up the beach (blue arrows in Figure 1c). These sediments are either supplied by strong tidal currents from Poole Harbour (red arrow in Figure 1c) or derive from cliff and dune erosion east of Bournemouth and at the northern tip of South Haven Peninsula (orange arrow in Figure 1c) [11]. Furthermore, sediment accumulation at the Peninsula also occurs by aeolian transport, forming dunes (green arrows in Figure 1c).

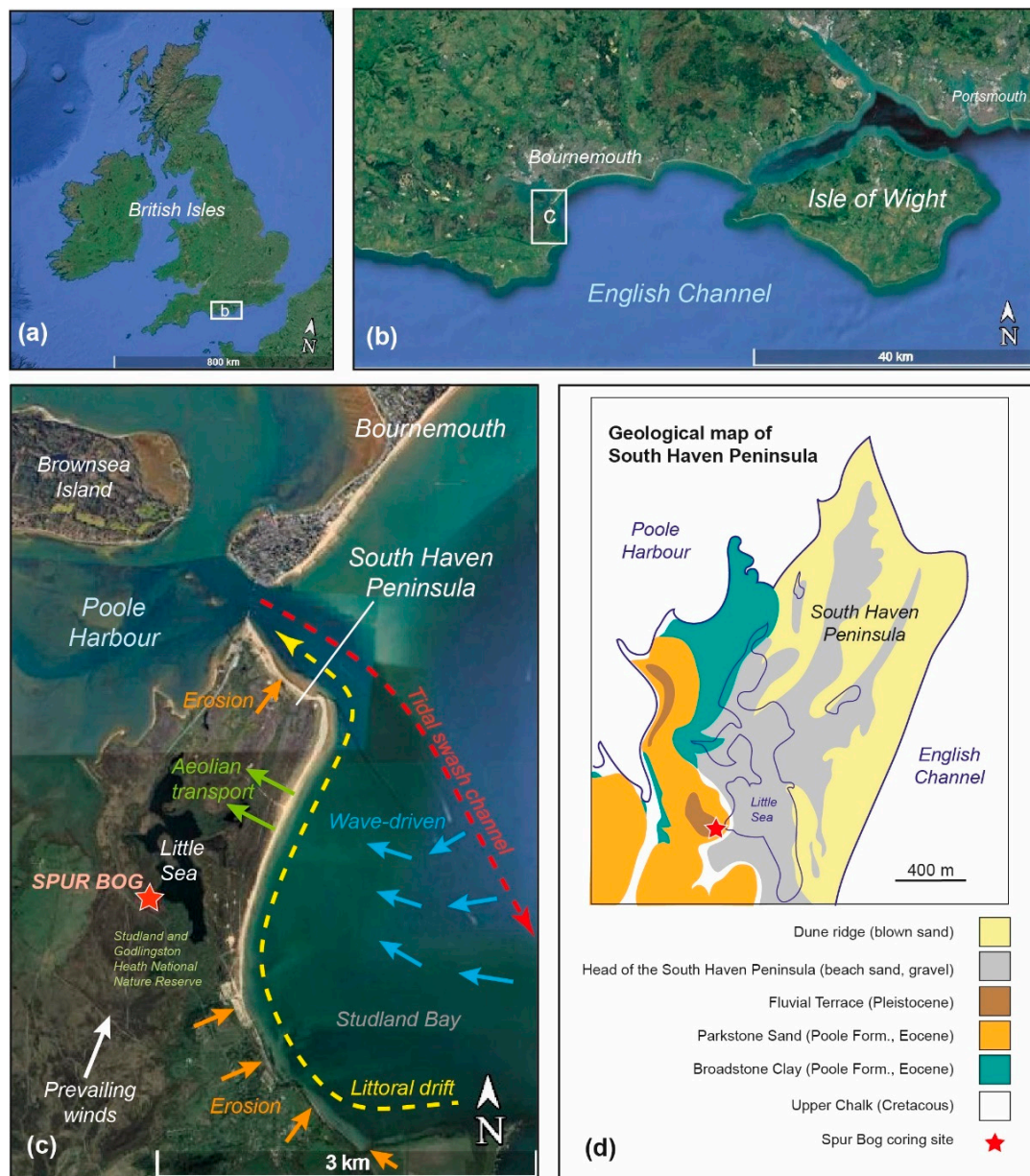


**Figure 1.** (a,b) Google Earth (2021) satellite images showing the study area in southern England. (c) Aerial image (Google Earth, 2021) of the South Haven Peninsula with the coring location at Spur Bog (red star). Coloured arrows indicate the main sediment transport processes in Studland Bay, based on the SCOPAC Sediment Transport Study [16], modified from [11]. (d) Geological map of South Haven Peninsula (modified from [14]).

### 2.2. Historical Records of the Geomorphological Developments of South Haven Peninsula

The earliest surviving contemporary depictions of the South Haven Peninsula date to the late 16th and early 17th centuries AD [17–21] (Figure 2). These sources depict the presence of a long, thin peninsula extending north easterly across Poole Harbour, with little evidence of sediment build up further east than its present-day western shore and no reference to the presence of freshwater bodies such as the Little Sea [6] (Figure 2a,b). Although no scale is defined within these sources, it is likely that the width of the peninsula ranges from 700 yards (640 m) at its widest to the south and <300 yards (<275 m) at its narrowest point protruding into Poole Harbour, whilst the vegetation status of the peninsula at this time is thought to have been predominantly heathland [6].

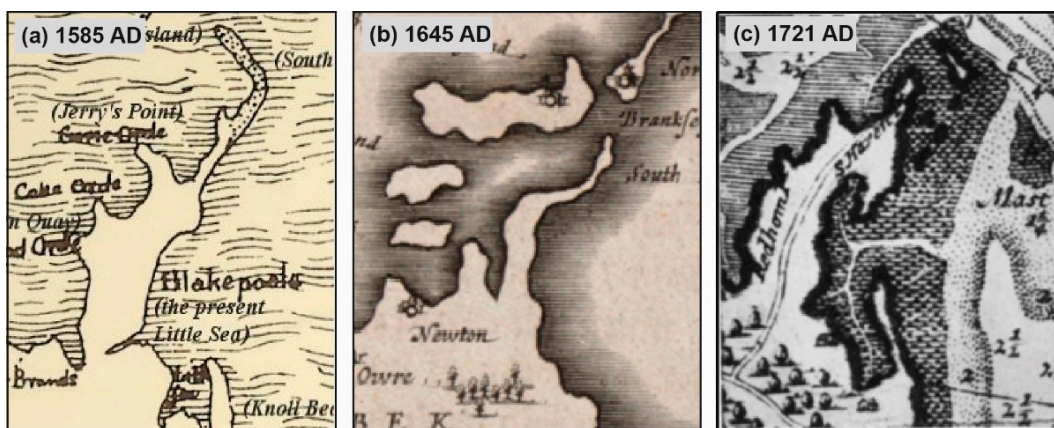


**Figure 2.** Physiological maps of the South Haven Peninsula during (a) the late 16th century AD [17]; (b) the mid-17th century AD [20,22]; (c) and the early 18th century AD [6,23].

Contemporary sources from the late 17th and early 18th centuries AD depict the formation of a wide, sandy beach along the eastern shore of the peninsula [24], whilst the development of additional dune ridges is noted behind Studland Beach and drainage channels running from the bay to an area shielded from Studland Bay by a thin sand bar protruding across the southern half of the inlet is evident in the work of [6,23] (Figure 2c). The aforementioned sand bar is approximated to be ~1000 yards (900 m) in length [6].

The development of this landform is further detailed during the late 18th century AD [25], by which time the beach had expanded eastward, becoming approximately half a mile (~800 m) wide [6] (Figure 3a). The system of drainage channels presented in the work of [6,23] appears to have developed into a lagoon, now referred to as ‘Little Sea’, which is noted to become inundated at high water due to the continued presence of drainage channels stretching from the lagoon into Studland Bay. The illustration by [26] of the South Haven Peninsula (Figure 3b) depicts further expansion of the South Haven Peninsula, including the development of an extensive dune system along the shore of the Little Sea and South Haven point. The expansion of these dune systems significantly encroaches upon Studland Beach, which is bisected by a sand ridge noted to be covered only at very high tide. The northern and southern halves of the Little Sea are split by a channel extending into Studland which facilitates tidal in-wash at high water, temporarily connecting these areas. Ecologically, the peninsula is characterised by dune environments in the west and heathland to the east, whilst marshland conditions are indicated around the Little Sea.

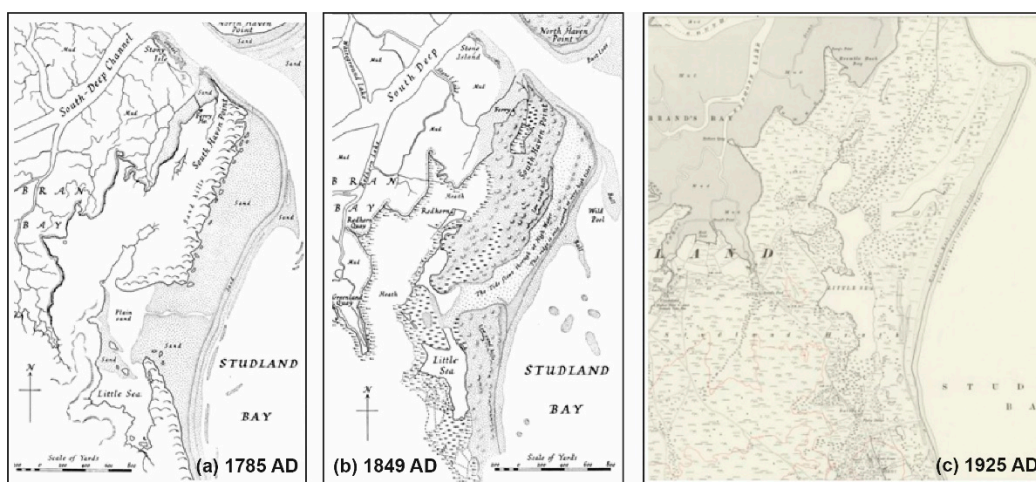


**Figure 3.** Physiological maps of the South Haven Peninsula during (a) the late 18th century AD [25]; (b) the mid-19th century AD [26], retrieved from Diver [6]; and (c) the early 20th century AD (1925 AD), retrieved from [27].

The study by Diver [6] notes significant geomorphological changes to the peninsula between the late 19th and early 20th centuries AD, including rapid erosion of the north-eastern tip of the peninsula, receding southward by 200 yards (180 m) between 1886 AD and 1924 AD (Figure 3c). In contrast, sediment accretion is noted along the eastern coast of the peninsula, resulting in eastward propagation out into Studland Bay by approximately 80 yards (72 m) during this time, attributed to the alteration of sediment transport pathways due to the construction of the Pier and coastal defences at Bournemouth [14]. Marked changes in environmental conditions are also noted within the interior of the South Haven Peninsula during this time, including in the reconnection of the northern and southern sectors of the Little Sea into a contiguous body of water totalling 35,400 m<sup>2</sup> by 1912 AD [6,10]. This lake was completely isolated from marine in-wash as a result of the aforementioned eastward propagation of the peninsula's eastern shore during the late 19th/early 20th centuries AD, with freshwater conditions (0.17 kg m<sup>-3</sup> NaCl) established within the Little Sea by 1932 AD [6]. Meanwhile, the formation of a further water body on the peninsula a short distance eastward of the Little Sea, referred to as 'Eastern Lake', is also noted to have occurred between 1894 AD and 1900 AD (Figure 3c).

Geomorphological changes to the South Haven Peninsula throughout the mid/late 20th and early 21st centuries AD are well documented as a result of extensive aerial photography of the area in addition to the monitoring of sediment accretion/erosion rates and the conduction of various geomorphological and ecological surveys [6,10,28–30]. These records evidence significant erosion of the north-eastern shores of the peninsula, recorded to be 0.5 m yr<sup>-1</sup> between 1933 AD and 1970 AD [31] and 0.4 m yr<sup>-1</sup> between 1951 AD and 2001 AD [32], contrasted by records of rapid sediment accretion along the south-eastern shore of the peninsula—ranging between 2.15 and 4.3 m yr<sup>-1</sup> (1936–1970 AD; [31]) and 1.12 to 2.43 m yr<sup>-1</sup> (1963–1970 AD; [33]). The interior of the peninsula also evidences significant geomorphological changes throughout the 20th century AD, including marked degradation of the dune systems to the east of the Little Sea as a result of military exercises, the construction of coastal defences and high levels of footfall [10], whilst a significant amount of WW2 era ordnance was dumped into the Little Sea [11]. Presently, the South Haven Peninsula is threatened by the disruption of sediment supply associated with the construction of Bournemouth Pier in the early 20th century AD [14] and relative sea level rise in the region [9,34,35].

### 2.3. Material and Methods

Fieldwork included transect mapping and coring and was carried out on Spur Bog in June 2018. A south-easterly transect consisting of twelve sampling points approximately one metre apart from one another was carried out across the centre of the bog using an auger gouger (Figure 4).

Of these sampling sites, transect point 4 (N 50°39'31.248'', W 001°57'46.512'') yielded the deepest gouger depth (132 cm) and thus was targeted for coring. Five contiguous, 10 cm overlapping sediment cores were taken at this transect point using a Russian Peat Corer of 50 cm length and a 6 cm diameter. A contiguous composite profile, SPUR-A, of 129 cm length was constructed for the sequence, excluding truncation of the sequence at 0–7 cm and 10–17 cm due to waterlogging (Figure 5). The cores were photographed, and the sedimentology was described prior to processing for multi-proxy analysis (loss on ignition (LOI), charcoal, pollen, humification, and grain size).

The composite profile SPUR-A was sub-sampled (~1 cm<sup>3</sup>) contiguously at 1 cm resolution (with the exception of the truncated sections at 0–7 cm and 10–17 cm) to quantify sediment organic matter content, achieved via LOI. Samples were dried in an oven at 105 °C for 24 h, then combusted in a furnace at 550 °C for 2 h with mass loss recorded between each step to enable the calculation of organic matter.

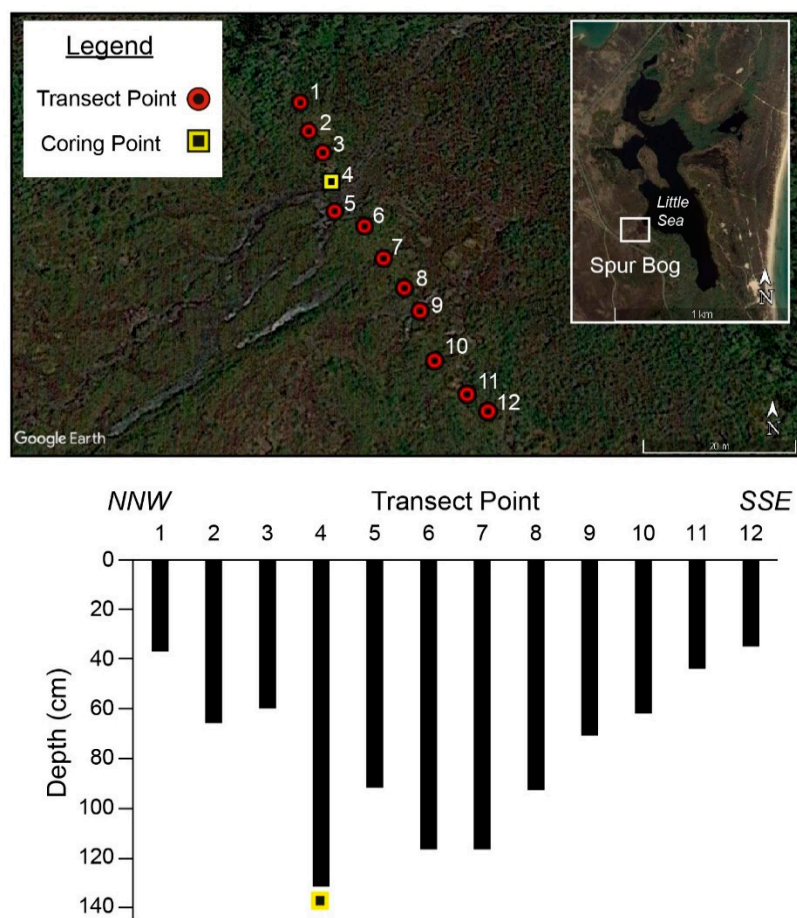


**Figure 4.** Location map of the NNW–SSE transect and sampling points of Spur Bog. The composite core SPUR-A has been taken from transect point 4 (yellow square).

The composite profile was additionally sub-sampled ( $\sim 1 \text{ cm}^3$ ) for pollen analysis to reconstruct vegetation changes at  $\sim 7 \text{ cm}$  resolution between 23 cm and 128 cm, with sampling in the upper 23 cm sequence limited by a lack of suitable material. Sample preparation was achieved following the standard extraction technique of sieving and acid digestion [36]. Processed samples were then mounted on microscope slides, and all pollen grains (56–563 grains per sample; see Supplement Table S1) were quantified and identified under a Zeiss transmitted light microscope at  $400\times$  and  $1000\times$  magnification to the lowest taxonomic level possible by morphology following [37] and comparison against reference collections available at the Physical Geography Laboratory of the School of Environment, Geography and Geosciences, University of Portsmouth. Raw pollen counts were categorised according to vegetation type (e.g., arboreal, dwarf shrub, herb and aquatic) and converted into relative abundance values for each taxon. Relative abundance assemblages were plotted stratigraphically using the ‘Rioja’ (v. 0.9–21) package for RStudio (v. 3.6.1) [38]. Following this, correlation analysis was performed to determine statistical relationships between microcharcoal, macrocharcoal, pollen concentration and pollen taxa to reconstruct sediment influx and ecosystem fire response (see Supplementary Table S1).

Down-core macrocharcoal and microcharcoal concentrations, defined as  $>125 \mu\text{m}$  and  $<125 \mu\text{m}$ , respectively [39], were quantified to reconstruct local sediment influx and fire regime. The composite sequence was sub-sampled ( $\sim 1 \text{ cm}^3$ ) contiguously in 1 cm increments between 20 cm and 129 cm and (where possible) between 0 cm and 20 cm for macrocharcoal analysis, whilst microcharcoal analysis was carried out using samples prepared during the aforementioned pollen analysis. Samples prepared for macrocharcoal analysis were sieved to remove material  $<125 \mu\text{m}$ , submerged in a sodium hypochlorite solution for five minutes, diluted and transferred to a gridded agar plate for counting. Counting

was completed at low magnification (10–20×) using a stereoscope, with macrocharcoal concentrations expressed as a raw count of total observed fragments. To account for variability in macrocharcoal concentrations due to sediment deposition flux, sedimentation rates ( $\text{cm yr}^{-1}$ ) were applied to raw macrocharcoal concentrations  $\text{cm}^{-3}$ , enabling the calculation of annual charcoal accumulation rates (CHAR, particles  $\text{cm}^{-2} \text{yr}^{-1}$ ).

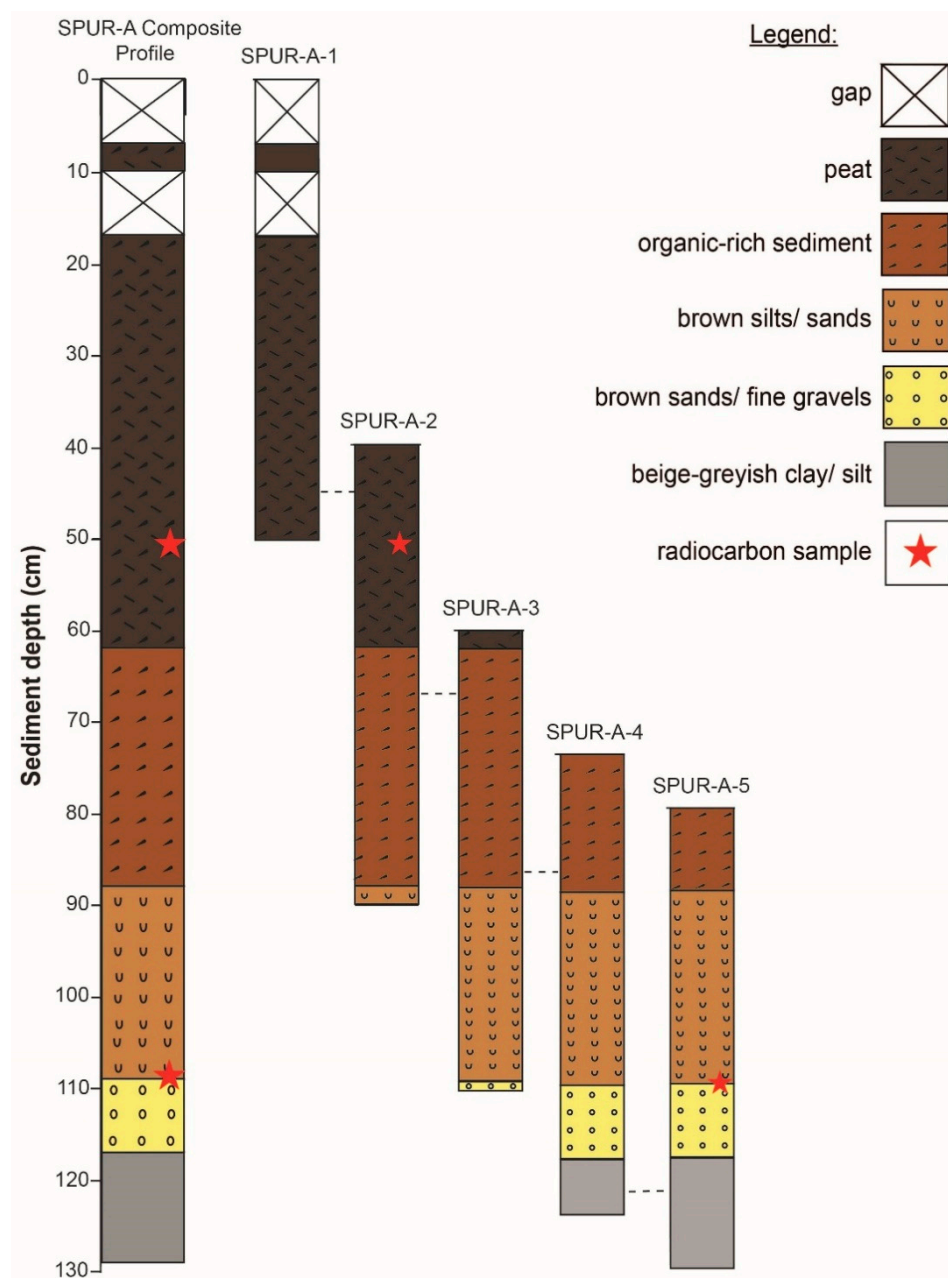


**Figure 5.** Lithology of composite profile SPUR-A, composed of five overlapping sediment cores SPUR-A-1 to SPUR-A-5 from Spur Bog, and positions of plant macrofossils sampled for radiocarbon dating.

Grain size analysis was carried out on detrital sediments of the composite profile contiguously between 109 cm and 128 cm at a resolution of 1 cm. Sub-samples of  $1 \text{ cm}^3$  were mechanically stirred in solution with deionised water and underwent laser diffraction analysis using a Malvern Mastersizer 3000 to quantify sediment grain sizes within each of the samples. The process was repeated on each sample three times, from which an average reading was calculated to reduce the effect of anomalous readings upon the dataset.

Humification analysis was limited to peat and organic-rich sections of the Spur Bog composite profile and undertaken at 10 cm resolution between the depths of 26 cm and

86 cm (Figure 5). The humification index (absorption value) has been obtained by using spectrophotometry, following the standard methodological process detailed in [40]. The measurement of each sample was repeated three times, from which an average absorbance value was calculated.

During sub-sampling of the composite profile for the aforementioned analyses, two plant macrofossils suitable for <sup>14</sup>C dating were extracted from the sequence at depths of 51 cm and 109 cm, respectively. These samples were analysed using Accelerator Mass Spectrometry (AMS) at Beta Analytic, Florida (USA). The AMS radiocarbon ages returned from this analysis were calibrated against the IntCal20 curve [41], whilst an age-depth model was developed using Bayesian modelling with OxCal v4.4.4 [42] (Table 1, Figure 6).

**Table 1.** AMS radiocarbon dates for samples extracted from the Spur Bog composite profile SPUR-A.

Sample ID	Material	Depth (cm)	<sup>14</sup> C Age (a BP), 2 σ Error	Calibrated Age (cal BP), 2 σ Error (Median)	Modelled Age (cal BP/cal AD)
Beta-507699	Wood macrofossil	51	130 ± 30	143 ± 135 (116)	250/1700 AD
Beta-501273	Wood macrofossil	109	860 ± 30	793 ± 104 (758)	740/1210 AD

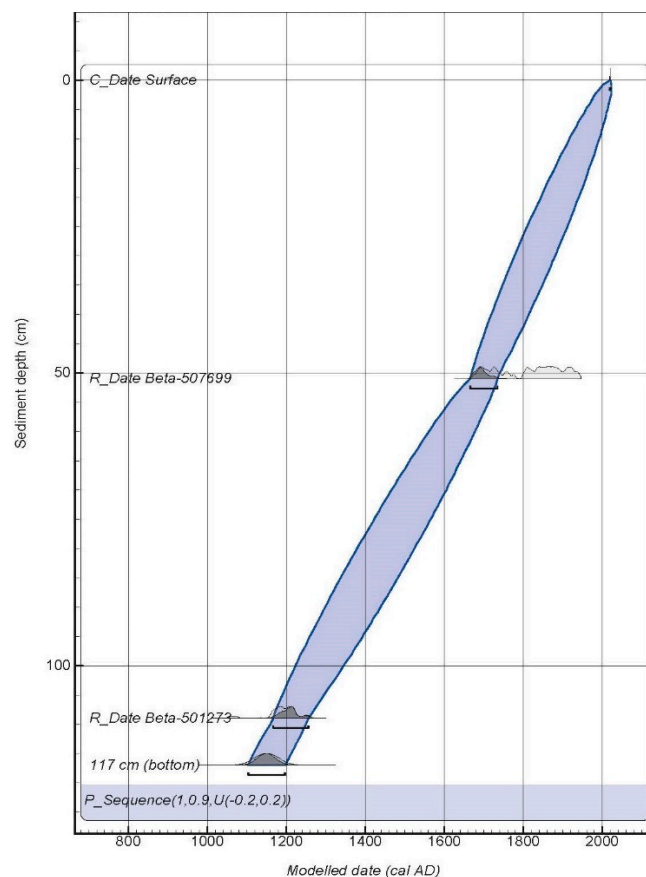


**Figure 6.** Bayesian age-depth model of composite profile SPUR-A from Spur Bog (excluding the Eocene clays at 117–129 cm depth). The model used the IntCal20 calibration curve [41] and the OxCal v4.4.4 software [42].

Detailed information of the age-depth model and multi-proxy raw data are provided in Supplementary Table S1.



### 3. Results

#### 3.1. Lithology

The composite profile SPUR-A is composed of clays, sands, silts, organic-rich sediments and peats (Figure 5). The basal sediments of the Spur Bog sequence (129–117 cm) consist of a beige-greyish claystone bedrock, identified as the Eocene Poole Formation—formerly ‘Bagshot Beds’ [12–14]. A sharp lithological boundary is visible at 117 cm, marked by the transition from claystone bedrock to brownish coarse sands and fine gravels which persist until 109 cm, where a diffuse transition towards brownish mixed silts and sands is noted. A second diffuse transition is noted at 88 cm from silts/sands to organic-rich sediments, followed by an abrupt transition to peats at ~62 cm depth. These peats persist throughout the remainder of the upper sequence with the exception of 17–10 cm and 7–0 cm, where the profile is truncated due to waterlogging.

#### 3.2. Chronology

The chronological framework for the Spur Bog sequence is based on interpolation using the two AMS radiocarbon dates of  $142 \pm 133$  cal BP (~1700 cal AD) and  $798 \pm 103$  cal BP (~1210 cal AD) at 51 cm and 109 cm composite depth, respectively (Table 1). The constructed age model (Figure 6) indicates that the deposition of sediments upon the Eocene Bagshot Bed Formation at 117 cm depth at the site likely began during the late Holocene at ~900 cal BP (~1150 cal AD). However, this age model does not consider the lithological changes at 109 cm from silts/sand to sand/gravel and at 117 cm from sands/gravel to the Eocene clays and silts, and hence the modelled ages below 109 cm composite depth only represent rough estimates which require further confirmation. According to the age model, the transition from silts/sands to organic-rich sediments at 88 cm composite depth is dated at  $\sim 550 \pm 100$  cal BP (~1390 cal AD  $\pm 100$  years), continuing until the deposition of peats  $\sim 340 \pm 100$  cal BP (~1610 cal AD  $\pm 100$  years) until the present day.

#### 3.3. LOI (Organic Matter Content)

LOI values within the basal Eocene clays (129–117 cm) are extremely low (<5%) and remain low (<10%) throughout the sand/gravel and silt/sand lithological layers within the lower sequence (117–88 cm depth, ~1150 to 1390 cal AD; Figures 6 and 7). A slight increase in LOI values to 15% is evidenced following the transition from silts/sands to organic-rich sediments at 88 cm (~1390 cal AD; Figures 6 and 7). LOI values increase steadily to 40% between 86 and 82 cm (~1400–1440 cal AD; Figures 6 and 7), followed by an abrupt decrease to 14% between 82 and 80 cm (~1440–1455 cal AD; Figures 6 and 7). At 79 cm (~1470 cal AD), LOI concentrations rebound quickly to 67% and remain relatively high (40–70%) throughout the remainder of the organic-rich sediment layer, with further peaks of 67–68% noted at 77–76 cm (~1480–1490 cal AD), 68 cm (~1560 cal AD), and 63 cm (~1600 cal AD; Figures 6 and 7). A further abrupt increase in LOI values to 80% occurs in the sequence at 62 cm depth (~1610 cal AD; Figures 6 and 7), corresponding to the lithological transition from organic-rich sediments to peats. LOI values are extremely high ~80–95% following this transition until 52 cm (~1610–1690 cal AD), before declining to 61% at 36 cm (~1800 cal AD; Figures 6 and 7). LOI values increase once again throughout the peaty sediments, recovering to ~90% prior to truncation of the sequence at 17 cm (~1910 cal AD; Figures 6 and 7).

#### 3.4. Pollen

The pollen assemblage of the Spur Bog profile is composed largely of *Pinus*, *Betula*, *Calluna*, *Poaceae* and *Sphagnum*, accounting for >80% of the total pollen (TP) grains within the sequence (Figures 7 and 8). Fluctuations in the pollen assemblage vary significantly throughout the sequence, indicating highly variable ecological conditions at the site in response to climate and environmental changes (Figures 7 and 8). Pollen assemblages of the Eocene bedrock are clearly distinguishable from those of historical sediments

(~1150–1880 cal AD) which can be further subdivided into five main pollen zones based solely on visual inspection (Figure 8).

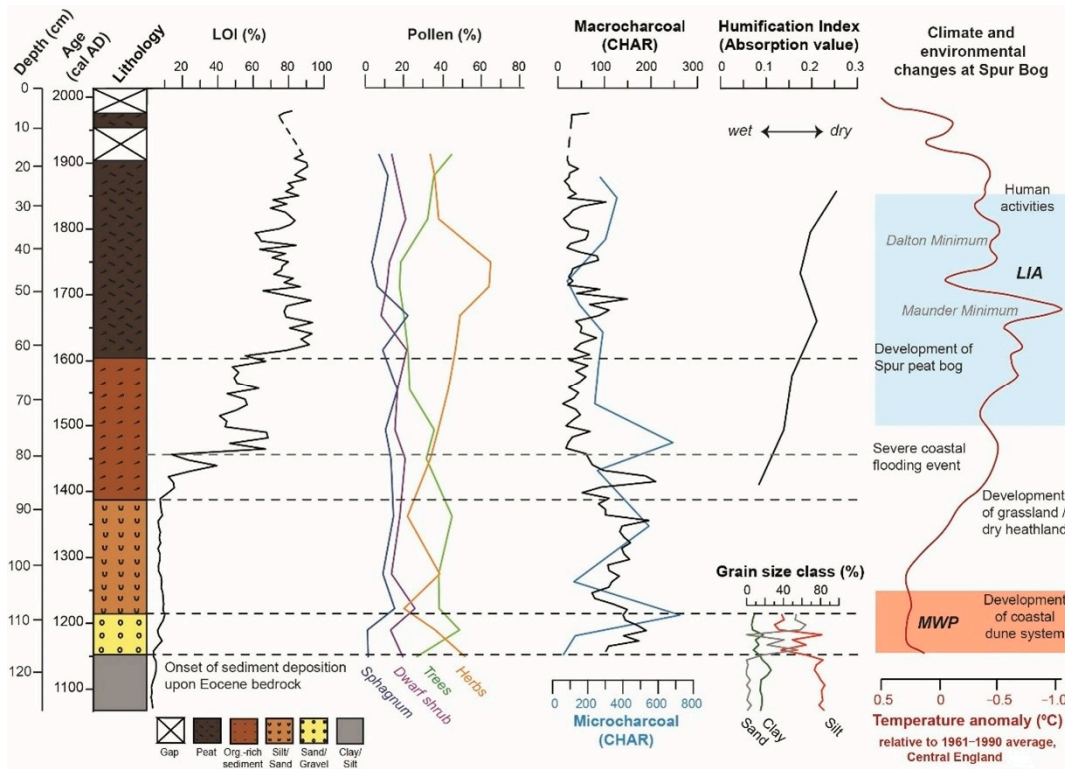


**Figure 7.** Lithology, loss of ignition (LOI), selected pollen species/groups data, charcoal, the humification index, and grain size data of Spur Bog core SPUR-A on a time scale and interpretation of multi-proxy data with regard to climatic and environmental changes (for detailed references, see Section 4.2). Dotted lines indicate major lithological changes. Abbreviations: LIA = Little Ice Age; MWP = Medieval Warm Period.

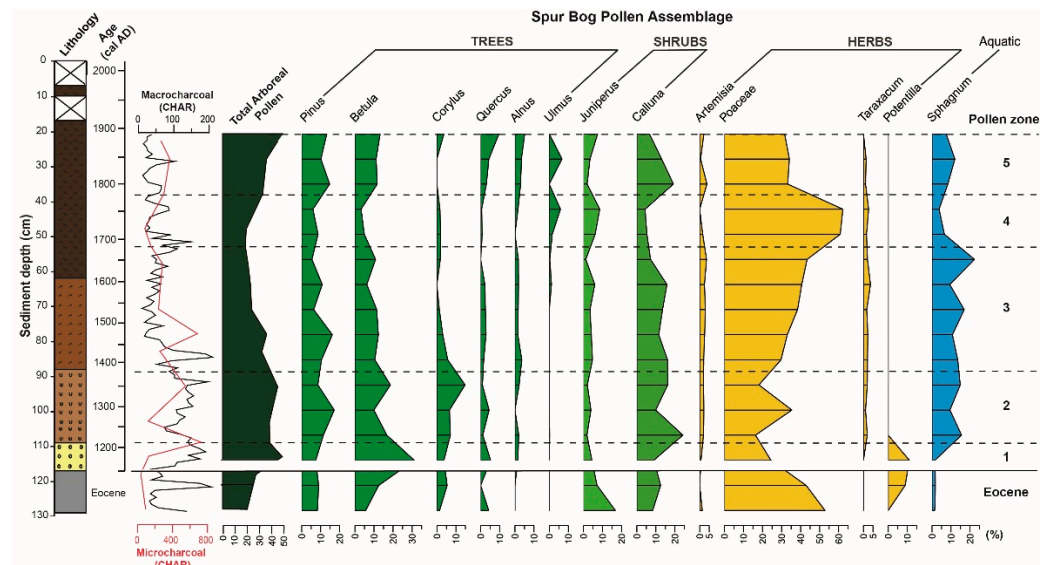


**Figure 8.** Pollen percentages of selected arboreal, shrub, herbaceous and aquatic pollen types in Spur Bog compared to lithology, total AP and macro- and microcharcoal fragment counts. See Figure 7 for the key of the lithological log.

#### 3.4.1. Eocene Bedrock (128–117 cm)

Eocene clays and silts are typified by extremely low pollen concentrations (<100 grains per cm<sup>3</sup>) and low species diversity. Arboreal pollen (AP) accounts for 19–27% of total pollen and is comprised of *Pinus* (8–9%), *Betula* (5–13%), *Corylus* (1–5%) and *Quercus* (0–4%). Dwarf shrub totals 20–25%, consisting of *Juniperus* (7–17%) and *Calluna* (8–13%), whilst herbaceous pollen is dominant at 52–54% due to high values of *Poaceae* (43–53%), *Potentilla* (9%) and low concentrations of *Artemisia* (0–1%). *Sphagnum* (1–2%) accounts for the remainder of the pollen total in this sediment.

#### 3.4.2. Pollen Zone 1 (117–109 cm; ~1150 to ~1210 cal AD)

Pollen zone 1 corresponds to the sand/gravel unit situated directly above the Eocene bedrock. In contrast to the Eocene clays, this zone evidences high levels of AP (49%), due the marked elevated values of *Betula* (31%), *Pinus* (7%), and *Corylus* (4%), and the establishment of *Quercus* (5%) and *Alnus* (2%). Subsequently, dwarf shrubs decline to 13% due to reduced concentrations of *Juniperus* (4%) and *Calluna* (9%). Herbaceous pollen consisting of *Poaceae* (24%), *Potentilla* (11%) and a low appearance of *Artemisia* (1%) decrease to 36%, whilst aquatic pollen species such as *Sphagnum* are sparsely present (2%).

#### 3.4.3. Pollen Zone 2 (109–88 cm; ~1210 to ~1390 cal AD)

Pollen zone 2 covers the entire sediment unit of brownish mixed silts and sands between 109 cm (~1210 cal AD) and 88 cm (~1390 cal AD). AP remains dominant, accounting for 38% of observed grains consisting of *Pinus* (11%), *Betula* (17%), *Corylus* (7%), and *Quercus* (1%). Dwarf shrub totals double to 26%, consisting largely of *Calluna* (24%) and just 2% of *Juniperus*. In contrast, herbaceous pollen totals are at their lowest value within the sequence (20%) due to the disappearance of *Potentilla*, the decline of *Poaceae* (16%) and low values of *Artemisia* and *Taraxacum* which makes its first appearance in the sequence (2%, respectively). Conversely, a significant increase in *Sphagnum* concentrations is noted, rising to 16% (Figures 7 and 8). Mid-zone 2 at ~1260 cal AD cm evidences marked changes in pollen concentrations. Whilst AP counts remain stable at 38%, the composition of arboreal species alters dramatically, with the expansion of *Pinus* (17%) and *Quercus* (4%) noted at the expense of *Betula* (10%), *Corylus* (7%) and *Alnus* which disappear from the record. Dwarf shrub pollen concentrations decrease to 14%, reflected in the decline of *Calluna* to 10%, while *Juniperus* values slightly increase to 4%. Herbaceous pollen totals increase to 39%, due to the expansion of *Poaceae* (35%) and the maintenance of *Artemisia* (2%) and *Taraxacum* (1%) species. Aquatic pollen, represented by *Sphagnum*, declines to 9%. The upper part of zone 2 at ~1350 cal AD evidences the highest AP values of the record (49%), consisting of *Pinus* (9%), *Betula* (19%), *Corylus* (15%), *Quercus* (1%), and *Alnus* (2%). Dwarf shrub values increase to 18%, comprised of *Juniperus* (2%) and *Calluna* (16%), whilst herbaceous pollen percentages decline sharply to 22% due to the reduction in *Poaceae* to 18% in addition to the stabilisation of *Artemisia* and *Taraxacum* at 2%, respectively. Conversely, *Sphagnum* recovers to 15%, comparable to its abundance at the beginning of the zone.

#### 3.4.4. Pollen Zone 3 (88–53 cm; ~1390 to 1680 cal AD)

Pollen zone 3 is the largest zone in the sequence, spanning from the transition from silts/sands to organic-rich sediments at 88 cm (~1390 cal AD) to the lower part of the peat unit at 53 cm depth (~1680 cal AD). A marked decline in AP totals from 45% to 32% is noted in this zone (Figure 7). The reduced AP values are associated with lower quantities of *Betula* (10%) and *Corylus* (6%), despite minor increases amongst *Pinus* (2%), *Quercus* (1%), and *Alnus* (2%). Dwarf shrub totals increase to 21%, reflecting increased *Juniperus* values (5%), whilst *Calluna* remains stable at 16%. Herbaceous pollen totals exhibit an increase from 22% to 34%, largely due to the expansion of *Poaceae* to 30%, becoming the dominant pollen type with *Artemisia* (2%) and *Taraxacum* (2%), and *Sphagnum* (14%) remaining relatively stable. Until ~1470 cal AD, AP values increase to 36%, corresponding to the expansion of *Betula* (12%), *Pinus* (16% TP) and *Quercus* (3%), counteracting declines

in *Corylus* (3%) and *Alnus* (2%). *Calluna* and *Juniperus* values decrease to 4% and 12%, respectively, resulting in reduced dwarf shrub pollen values (16%). Herbaceous species to become the dominant vegetation type (38%) as *Poaceae* values increase further to 33% with *Artemisia* (2%) and *Potentilla* (1%) retain marginal species, whilst *Sphagnum* declines to 11%. The upper part of zone 3 (~1470–1680 cal AD) shows a gradual decline in AP values from 36% to 20% consisting largely of *Pinus* and *Betula* (16% in total), in addition to marginal (>2%) populations of *Corylus*, *Quercus*, *Alnus* and *Ulmus*, appearing for the first time in the record. Dwarf shrub totals vary throughout upper zone 4, initially rising to 22% (*Juniperus* 6%, *Calluna* 16%), before declining to a minimum value of 8% (*Juniperus* 1%, *Calluna* 7%) prior to the zone 3/4 boundary. In contrast to AP, herbaceous pollen evidences a gradual increase from 38% to 49%. This is driven by a rise in *Poaceae* values from 33% to 43%, whilst *Artemisia* and *Taraxacum* values fluctuate between 2% and 4%. *Sphagnum* retains moderate values throughout this zone before rising to a maximum value of 22% at the transition to zone 4, exhibiting an inverse relationship with dwarf shrub concentrations (Figure 8).

#### 3.4.5. Pollen Zone 4 (53–38 cm; ~1680 to 1780 cal AD)

Pollen zone 4, situated in the lower to middle part of the peat unit, is characterised by extremely low AP concentrations (<20%), comprised largely of *Pinus* (9%) and *Betula* (5%), alongside low (<2%) concentrations of *Corylus*, *Quercus* and *Ulmus* in lower zone 5, whilst in upper zone 4 AP values consist of *Pinus* (6%), *Betula* (3%), *Ulmus* (6%) and low values (<2%) of *Corylus*, *Quercus* and *Alnus*. Dwarf shrub values recover to 12% throughout zone 4, owing to the expansion of *Juniperus* (9%) despite the decline of *Calluna* (4%). A marked increase in herbaceous pollen totals occurs within this zone, increasing to 65% due to the rise in *Poaceae* to 61%, whilst *Artemisia* and *Taraxacum* account for the remaining 4%. Conversely, an abrupt decrease in *Sphagnum* pollen is noted, declining from 22% at the onset of zone 4 to 4% at the zone 4/5 boundary at ~1780 cal AD.

#### 3.4.6. Pollen Zone 5 (43–23 cm; ~1780 to 1880 cal AD)

Pollen zone 5 is the youngest zone in the record, pertaining to the middle to upper parts of the peat unit prior to truncation of the sequence. This zone evidences the recovery of AP values, becoming the dominant pollen type at the upper bound of the zone (45%) due to the expansion of *Pinus* (13%), *Betula* (13%), *Quercus* (9%), *Alnus* (5%), and the reappearance of *Corylus* (4%). This is contrasted by dwarf shrub values, which decline from 21% (*Juniperus* 2%, *Calluna* 19%) to 14% (*Juniperus* 7%, *Calluna* 7%) throughout zone 5. An abrupt decrease in herbaceous pollen also occurs at the transition of zones 4 and 5 from 65% to 38% due to the decline of *Poaceae* (33%) and *Taraxacum* (1%), despite the reappearance of *Artemisia* (4%). Throughout zone 5, herbaceous pollen continues to decline gradually to 34%, as *Poaceae* and *Artemisia* fall to 32% and 2%, respectively, whilst *Taraxacum* disappears from the record. *Sphagnum* values fluctuate throughout zone 5, initially recovering to 12% before declining to 7% at the top of the zone.

### 3.5. Macro- and Microcharcoal

Similar to pollen assemblages, macro- and microcharcoal concentrations within the Spur Bog sequence exhibit significant variability (Figures 7 and 8). Macrocharcoal and microcharcoal concentrations in the basal Eocene clays (129–117 cm) are generally low (<70 and <100 fragments per cm<sup>-3</sup>, respectively), with macrocharcoal excursion peaks at 129 cm (136 fragments cm<sup>-3</sup>), 122 cm (175 fragments per cm<sup>-3</sup>) and 121 cm depth (205 fragments cm<sup>-3</sup>).

Macrocharcoal concentrations increase significantly within pollen zone 1 (117–109 cm; ~1150–1215 cal AD), with concentrations >100 fragments cm<sup>-3</sup> (~5.5 cm<sup>-2</sup> yr<sup>-1</sup>) of macrocharcoal observed throughout this zone, rising to between 140 and 190 fragments per cm<sup>-3</sup> (7.5–10 cm<sup>-2</sup> yr<sup>-1</sup>) throughout the middle and upper part of zone 2 (114–109 cm; ~1170–1215 cal AD). Similarly, microcharcoal concentrations increase to 129 fragments cm<sup>-3</sup> in the middle of

zone 2 (113 cm; ~1180 cal AD) and 724 fragments  $\text{cm}^{-3}$  at the zone 2/3 boundary (109 cm; ~1215 cal AD) (Figures 7 and 8).

Within pollen zone 2 (109–88 cm; ~1215–1390 cal AD), macrocharcoal concentrations are variable, initially remaining at levels comparable to upper zone 1 ( $>100$  fragments  $\text{cm}^{-3}$ ,  $\sim 7 \text{ cm}^{-2} \text{ yr}^{-1}$ ) between 109 cm and 107 cm (~1215–1230 cal AD), before falling to  $< 80$  fragments  $\text{cm}^{-3}$  ( $< 4 \text{ cm}^{-2} \text{ yr}^{-1}$ ) between 106 cm and 105 cm (~1240–1250 cal AD). Macrocharcoal concentrations increase to  $\sim 110$  fragments  $\text{cm}^{-3}$  ( $\sim 5.5 \text{ cm}^{-2} \text{ yr}^{-1}$ ) within the middle of zone 2 (104–100 cm; ~1260–1290 cal AD), with a minor peak of 132 fragments  $\text{cm}^{-3}$  ( $6.5 \text{ cm}^{-2} \text{ yr}^{-1}$ ) recorded at 102 cm depth (~1270 cal AD). Following this, macrocharcoal concentrations increase throughout the middle and upper part of zone 2 (99–92 cm; ~1300–1360 cal AD), exceeding 130 fragments  $\text{cm}^{-3}$  ( $> 6.5 \text{ cm}^{-2} \text{ yr}^{-1}$ ) and peaking at 196 fragments  $\text{cm}^{-3}$  ( $9.6 \text{ cm}^{-2} \text{ yr}^{-1}$ ) at 92 cm (~1360 cal AD). Macrocharcoal concentrations decline sharply thereafter to  $\sim 100$  fragments  $\text{cm}^{-3}$  ( $\sim 5 \text{ cm}^{-2} \text{ yr}^{-1}$ ) in the upper part of zone 2. In comparison, microcharcoal concentration in lower zone 3 is low (121 fragments  $\text{cm}^{-3}$  at 103 cm; ~1260 cal AD) before rising in the middle to upper part of zone 2 to 548 fragments  $\text{cm}^{-3}$  (93 cm; ~1350 cal AD) in phase with macrocharcoal (Figures 7 and 8).

A decrease in macrocharcoal concentrations to  $\sim 50$  fragments  $\text{cm}^{-3}$  ( $2.5 \text{ cm}^{-2} \text{ yr}^{-1}$ ) is noted immediately above the pollen zone 2/3 boundary at 87 cm (~1400 cal AD). Following this, a significant peak in macrocharcoal concentrations of  $\sim 200$  fragments  $\text{cm}^{-3}$  occurs between 85 cm and 84 cm (~1410–1420 cal AD). Throughout the remainder of pollen zone 4 (83–53 cm; ~1430–1680 cal AD), macrocharcoal concentrations remain low (10–98 fragments  $\text{cm}^{-3}$ ). In contrast, charcoal accumulation rates are highly variable throughout zone 4, ranging from  $45 \text{ cm}^{-2} \text{ yr}^{-1}$  within the aforementioned peak in the lower part of zone 4 to  $2.3 \text{ cm}^{-2} \text{ yr}^{-1}$ . Microcharcoal concentrations within zone 3 are moderate (240–286 fragments  $\text{cm}^{-3}$ ), with an excursion peak of 684 fragments  $\text{cm}^{-3}$  noted at 78 cm depth (~1470 cal AD) (Figures 7 and 8).

The upper part of pollen zone 3 and the lower part of pollen zone 4 (55–50 cm; ~1660–1710 cal AD) exhibit significant variability in macrocharcoal concentrations, with peaks of 110, 149 and 90 fragments  $\text{cm}^{-3}$  ( $26$ ,  $35$  and  $21 \text{ cm}^{-2} \text{ yr}^{-1}$ ) at ~1670, ~1680, ~1690 and 1710 cal AD, respectively, interspersed by lower counts of  $68 \text{ cm}^{-3}$  and  $40 \text{ cm}^{-3}$ . Macrocharcoal concentrations in upper zone 4 (49–44 cm; ~1710–1740 cal AD) fall to low, stable values between 21 and 32 fragments  $\text{cm}^{-3}$  before rising to 55 fragments  $\text{cm}^{-3}$  at the zone 4/5 boundary. Microcharcoal concentrations decline throughout zone 4 to  $153 \text{ cm}^{-3}$  (53 cm; ~1680 cal AD) and  $83 \text{ cm}^{-3}$  (48 cm; ~1720 cal AD) (Figure 7). The lower zone 4 exhibits similar low macrocharcoal concentrations ( $< 50$  fragments  $\text{cm}^{-3}$ ,  $< 10 \text{ cm}^{-2} \text{ yr}^{-1}$ ). However, macrocharcoal peaks of  $> 80$ , 65 and 103 fragments  $\text{cm}^{-3}$  ( $20$ ,  $15$  and  $24 \text{ cm}^{-2} \text{ yr}^{-1}$ , respectively) are evident at 43–42 cm (~1750–1760 cal AD) and immediately following the zone 4/5 transition at 38 cm–36 cm (~1780–1790 cal AD) and 29 cm (~1840 cal AD), respectively.

The upper pollen zone 5 (28–23 cm; ~1840–1880 cal AD) reveals low macrocharcoal concentrations (14–39 fragments  $\text{cm}^{-3}$ ,  $< 10 \text{ cm}^{-2} \text{ yr}^{-1}$ ) comparable to the rest of zone 5 and upper zone 4 (Figures 7 and 8).

### 3.6. Grain Size

Sediment grain sizes within the lower sequence (128–109 cm) evidence multiple changes to the type of sediments deposited at the site (Figure 7). Within the basal Eocene clays (128–117 cm), mean sediment grain sizes are within the clay and fine silt fraction ( $< 10 \mu\text{m}$ ) and maximum grain sizes typically do not exceed  $250 \mu\text{m}$ , indicating a low-energy depositional environment. In contrast, mean sediment grain sizes of the overlying historical sediments at 117 cm depth (~1150 cal AD; Figures 6 and 7) increase to  $< 12 \mu\text{m}$  and maximum grain size increases significantly to  $> 2000 \mu\text{m}$ . Sediment grain size remains relatively stable between 117 cm and 114 cm (~1150–1174 cal AD; Figures 6 and 7), consisting mainly of silts and fine sands (mean grain sizes of  $\sim 10$ – $30 \mu\text{m}$ ). This is followed by an abrupt

increase in sediment grain sizes to  $>90\ \mu\text{m}$  (mean) and  $>500\ \mu\text{m}$  (maximum) between 112 and 109 cm ( $\sim 1190\text{--}1215$  cal AD; Figures 6 and 7).

### 3.7. The Humification Index

Humification indices have been obtained for organic-rich sediments and peats between 86 and 26 cm depth ( $\sim 1410\text{--}1860$  cal AD; Figures 6 and 7) to document the development of the bog and to determine natural climate processes (wetness/dryness) at the site (Figure 7). The lowermost sample at 86 cm depth has a spectral absorption value of 0.084%, and levels rise continuously to up to 0.211% throughout the remainder of the organic-rich sediments and into the peat layer at 56 cm depth ( $\sim 1660$  cal AD), indicating a relatively constant increase in humification of deposited organic material. This increase in humification occurs synchronously to a marked increase in LOI values from 15% at  $\sim 1390$  cal AD to a maximum value of 93% by 1660 cal AD. Humification levels slightly regressed throughout the late 17th and early 18th centuries AD, evidenced by a spectral absorption value of 0.175% at 46 cm depth ( $\sim 1730$  cal AD). Humification levels constantly increased again during the late 18th and mid-19th centuries AD, evidenced by absorption values of 0.197% at 36 cm ( $\sim 1795$  cal AD) and 0.254% at 26 cm depth ( $\sim 1860$  cal AD).

## 4. Discussion

### 4.1. Relationships between Pollen Taxa and Wildfire Regime

Microcharcoal concentrations observed within the Spur Bog sequence exhibit a significant positive correlation with pollen grain concentrations ( $r^2 = 0.88$ ), reflecting the potential for these proxies to capture variations in climatic variables (e.g., temperature, precipitation, and aeolian processes) and their impact upon the deposition of organic material. The analysis of statistical relationships between respective pollen taxa, microcharcoal and macrocharcoal evidences marked variation between the development and maturation phases of the site (Figure 9). Macrocharcoal and microcharcoal concentrations exhibit positive to strong positive correlation with all pollen taxa (with the exception of *Quercus* and *Potentilla-microcharcoal only*), indicating that the deposition of charcoal fragments and most pollen taxa during the developmental phase of the site occurred simultaneously during high-energy depositional events (e.g., coastal flooding) [43]. In contrast, pollen/charcoal abundance relationships during the maturation phase of the Spur Bog exhibit clear variations according to vegetation type. Arboreal pollen types respond positively ( $r^2 = 0.45\text{--}0.87$ ) to microcharcoal—excluding *Ulmus* ( $r^2 = -0.26$ )—and neutral-negatively ( $r^2 = 0\text{--}0.45$ ) with macrocharcoal—with the exception of *Corylus* ( $r^2 = 0.20$ ). Non-arboreal pollen types are also positively correlated with microcharcoal ( $r^2 = 0\text{--}0.54$ ) and, to a lesser extent, macrocharcoal ( $r^2 = 0.06\text{--}0.18$ )—with the exception of *Sphagnum* ( $r^2 = -0.06$ ). This indicates that the mechanisms associated with microcharcoal deposition at the Spur Bog are also conducive to the deposition of pollen—particularly species adapted for long-distance pollen dispersal, *Pinus* and *Betula*—whilst the negative relationship between macrocharcoal and arboreal pollen indicates that fire events (natural or otherwise) inhibited the development of woodland species, with the notable exception of *Corylus* due to its adaptation for post-fire recolonisation [44,45]. In contrast, dwarf shrub and herbaceous pollen types responded positively to macrocharcoal concentrations due to its association with fire events and human activity which prevent ecological succession. The weak negative relationship between *Sphagnum* and macrocharcoal suggests that climatic conditions had a negligible effect on the frequency and intensity of fire events, thus presenting human activity as the main driver of the site's fire regime.

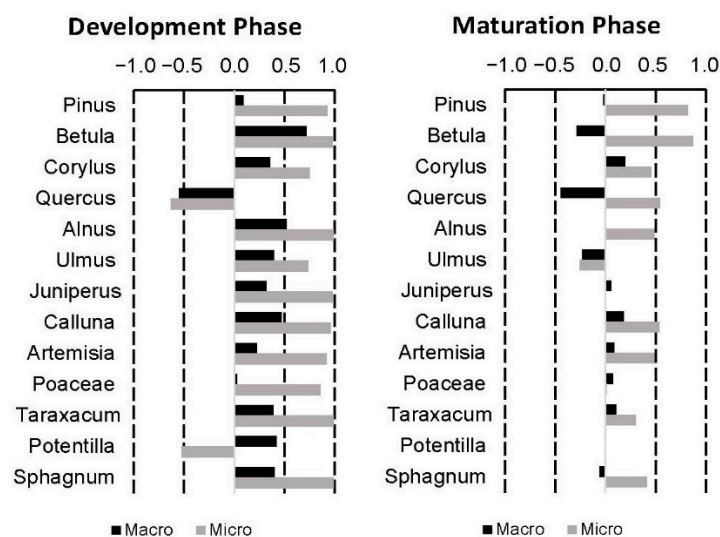


**Figure 9.** Statistical relationship between the abundance of pollen taxa and macro-/microcharcoal fragment frequency during the development (left panel) and maturation (right panel) of the Spur Bog. See Supplementary Table S1 for further details.

#### 4.2. Climate and Environmental Changes at Spur Bog since ~1150 cal AD

Based on the age-depth model, deposition of young (historical) sediments upon the Eocene bedrock at Spur Bog started at ~1150 cal AD, during the ‘Medieval Warm Period’ (MWP). The basal coarse-grained, inorganic sediments (gravel/sands) indicate a high-energy coastal depositional environment at that time, possibly influenced by flooding during severe storm events recorded in the southern North Sea and the English Channel in 1134 AD and/or 1178 AD [46], both of which fall within the  $2\sigma$  uncertainty range of the Spur Bog age-depth model (Figure 6). Pollen assemblages of zone 1 between ~1150 and 1210 cal AD reflect a typical brackish coastal dune environment with sparse pioneer communities of *Calluna*, *Poaceae* and *Sphagnum*, and distal arboreal pollen most likely deposited by marine processes. High amounts of macro- and microcharcoal fragments support this hypothesis. The rapid deposition of inorganic, marine-derived sands between ~1190 and 1210 cal AD possibly indicates that the initial development of the South Haven Peninsula was associated with an extreme high-energy depositional environment, consistent with extensive coastal flooding in the region between 1200 and 1219 AD noted in contemporary records [47,48].

At ~1210 cal AD, at the onset of pollen zone 2, the marked variation in pollen assemblage occurs simultaneously to the lithological transition from coarse sands to finer silts and sands and an increase in LOI to 15%, thus presenting strong evidence of abrupt environmental changes. These changes are interpreted as the decline in marine influence at the site as the South Haven Peninsula continued to develop, facilitating the establishment of a brackish coastal floodplain environment populated by typical pioneer communities of *Calluna*, *Poaceae* and *Sphagnum*, which are indicative of less saline conditions [49–51]. High volumes of arboreal pollen and macro- and microcharcoal fragments, which are interpreted as having a larger, regional source during this time, as well as low LOI values indicate continued periods of inorganic sediment input, possibly deposited as a result of coastal flooding events recorded during the first half of the 13th century AD [46,48,52,53]. Between ~1250 and 1390 cal AD, at the termination of the MWP, pollen assemblages at Spur Bog indicate an increasingly brackish environment but strongly influenced by marine processes. This is supported by the stagnation of LOI values at ~7% and contemporary records of severe storm surge events affecting south-eastern England during 1362 AD and 1374–1375 AD [46,53].

A significant reduction in the influence of coastal processes upon the Spur Bog is visible from the pollen record (zone 3) starting at ~1390 cal AD, facilitating the establishment of grassland and wet heathland environments consisting of *Juniperus*, *Calluna*, *Poaceae*

and *Sphagnum*. This interpretation is supported by the lithological transition from silts to organic-rich sediments between ~1390 cal AD and 1430 cal AD (Figure 7). Pollen changes at ~1470 cal AD present strong evidence for the development of a mature terrestrial environment devoid of marine influences, resulting in the establishment of wet heathland, dry heath, and grassland near Spur Bog which was likely facilitated by sheltering of the site by a coastal landform (e.g., sand bar and dune system). Furthermore, reduced local wildfire activity is inferred by the rapid decrease in macrocharcoal fragments at ~1430 cal AD. Climatic amelioration in the region throughout the late 15th century AD [53,54] also facilitated the development of medial-distal woodlands possibly located south from Spur Bog.

Between ~1490 and 1550 cal AD, cooler/wetter conditions resulted in the decline of nearby woodland environments and subsequent expansion of grassland and wet heathland at Spur Bog, which is also evidenced by a notable decrease in LOI values (Figure 7). The climatic deterioration inferred from the Spur Bog record conforms strongly to contemporary accounts from southern England which detail cold winters, wet summers and frequent coastal storms throughout the 16th century AD [46–48,52,53], typically associated with the onset of the ‘Little Ice Age’ (LIA) cooling period experienced across Europe at ~1500 AD [55,56]. Low wildfire activity at the Spur Bog and surrounding area during the late 15th and 16th centuries AD, evidenced by reduced macro- and microcharcoal fragment counts, are furthermore indicative of the climatic deterioration identified across Britain and north-western Europe during the early LIA [57–59]. Climatic conditions lasted at Spur Bog until ~1610 cal AD as supported by continuing decreasing arboreal pollen and increasing *Poaceae* concentrations and stagnating values in LOI (Figures 7 and 8). The onset of peat deposition at that time indicates the establishment of a terrestrial wetland environment at Spur Bog.

The pollen record at the transition of zone 3 and 4 (~1670–1700 cal AD) presents strong evidence of a vegetation succession from wet heath to a dry heath/grassland and further decline of woodland, consistent with a proposed cold and arid climate as also implied by high peat humification values and macrocharcoal counts (Figure 7). Contemporary evidence suggests that southern England experienced a prolonged period of extremely cold conditions throughout the mid- and late 17th century AD [60–63], including a period of drought between 1684 and 1686 AD [44,49,50,54], which coincided with the ‘Maunder Minimum’ of the LIA. However, the possibility of anthropogenic activity impacting upon environmental conditions at the site cannot be discounted, due to the intensive removal of peat and timber from southern England for fuel, building materials and agricultural practices throughout the 16th, 17th and early 18th centuries AD [64–67].

At ~1720 cal AD, a climatic shift towards warmer and likely slightly wetter conditions following the ‘Maunder Minimum’, conforming with increasing arboreal pollen taxa (zone 4) and decreased peat humification values and reduced wildfire activity observed in the Spur Bog sequence and regional climate records at this time [47,52,53,68,69]. Elevated macrocharcoal counts between ~1750 and 1760 cal AD coincide with unusual warm and dry conditions during October 1752 AD and July 1757 AD [53,70], which could have facilitated a natural fire event near Spur Bog. Alternatively, these charcoal peaks could reflect anthropogenic activities, such as arson [71] or land reclamation [67].

The marked shift in the pollen record at ~1780 cal AD (the onset of zone 5) of the Spur Bog suggests vegetation succession towards mixed woodland and reduced grassland and wet heathland communities, indicating drier climatic conditions corroborated by increasing peat humification values and elevated macrocharcoal counts at Spur Bog as well as historical records from the region [47,52,70,72,73]. This period coincides with the ‘Dalton Minimum’ of the LIA which was characterised by general cooler winters and variable dry and wet summers in England [47,52,53]. It also coincides with the intensification of agricultural and industrial activities in the region, resulting in the clearance of one quarter of all heathland habitats within the Poole Basin between 1760 AD and 1811/17 AD to facilitate the construction of roads, livestock grazing and planting of Pine forests [72–74].



The pollen assemblage exhibits climatic amelioration during the early-mid 19th century AD, facilitating the expansion of mixed woodland and wet heathland communities at the Spur Bog. These vegetation changes occur simultaneously to a period of relatively high mean temperatures and increased precipitation between 1830 AD and 1860 AD [69], further supported by reduced fire activity at Spur Bog (Figures 7 and 8) and instrumental records detailing prolonged warm, wet conditions throughout the winter of 1845/46 AD and summer of 1846 AD in the region [47,52,75]. A macrocharcoal peak at ~1840 cal AD may be either in response to exceptional dry conditions recorded during 1834/35 AD or 1840 AD [53,70,74] or reflect anthropogenic activity.

The encroachment of mixed woodland at the Spur Bog facilitated by a warmer, wetter climate in England following the end of the LIA at ~1850 AD [53,70,76,77] is supported by contemporary historical records, which document the expansion of the '12 Acre Wood' and other woodlands within the Poole Basin, facilitated by the decline of livestock grazing and peat/furze cutting in the region [6,73]. Throughout the late 19th century AD, generally low, stable macrocharcoal concentrations are exhibited, corresponding to a period of relatively low temperatures and wet summers in the region [69,70]. Two notable charcoal peaks occur at ~1890 AD and ~1976 AD during periods of hot, dry summers [69,70,78]—the former of which may be linked to the fire which damaged Brownsea Castle in 1896 [79,80].

#### 4.3. Geomorphological Changes of the South Haven Peninsula since ~1150 cal AD

The aforementioned reconstruction of climatic and environmental conditions at the Spur Bog reveals that ecological and geomorphological changes at the South Haven Peninsula have been extremely rapid during the last ~900 years (Figure 10).

Sediment accretion at the site is thought to have begun at ~1150 cal AD, associated with the deposition of coarse sands and fine gravels observed in the Spur Bog record. It is hypothesised that these sediments have been deposited in a coastal environment, i.e., within the intertidal zone (Figure 10a), which is also supported by low organic matter content and high concentrations of distally transported arboreal pollen and charcoal fragments. This type of environment is indicative of a marked shift in regional sediment transport pathways, enabling the formation of a sand-bar around which further sediment coalesced over time as proposed by [6,10,81]. The development of such a landform was likely facilitated by a period of relative sea level fluctuation around Poole Harbour, resulting in a period of enhanced sediment deposition in the region between 750 AD and 1150 AD [9], the timing of which correlates closely with the ~1150 cal AD age attributed to the basal sands and gravels of the Spur Bog sequence.

The lithological transition between sands/gravels and silts/sands in the Spur Bog core at ~1210 cal AD is interpreted as a decline in marine sediment supply, which is in accordance with the proposed reduced marine sediment deposition in the area at ~1150 AD likely as a result of eastward propagation of the peninsula into the English Channel [9], and hence general lower-energetic depositional conditions at Spur Bog (Figure 10b). This type of environment is corroborated by increased concentrations of dwarf shrub, herbaceous and aquatic pollen taxa in the Spur Bog sequence, in contrast to reduced arboreal pollen taxa and macrocharcoal concentrations between ~1210 and 1270 cal AD. Throughout the late 13th and the entire 14th century AD, continuously high macrocharcoal concentrations and the presence of saline tolerant pollen taxa indicate that the site continued to be significantly influenced by marine processes, i.e., by frequent coastal flooding, which prevented further ecological succession.

The diffused boundary within the Spur Bog sequence between silts/sands to organic-rich sediments at ~1390 cal AD, which is accompanied by a slight increase in bioproductivity and marked reduction in distally transported arboreal pollen and charcoal fragment concentrations, is indicative of the development of a wetland environment at the site which is possibly protected by a sand bar or a developing dune system (Figure 10c). This resulted in the decreased influence of marine-coastal processes due to further gradual sediment accretion around this landform and subsequent eastward propagation of the peninsula.

Severe coastal flooding events at ~1420 AD and ~1460 AD are inferred from abrupt decreases in organic matter and elevated macrocharcoal concentrations, evidencing continued vulnerability of the Spur Bog to the intense coastal storm activity which is documented throughout the early 15th century AD across north-western Europe [46–48,82]. This period is followed by a cessation of marine influence upon the site. Higher levels of bioproductivity associated with a fully established terrestrial environment at Spur Bog (Figure 10d) are evidenced between ~1470 cal AD and 1610 cal AD. This is supported by high concentrations of *Calluna*, *Poaceae* and *Sphagnum* pollen associated with wet heathland, dry heathland and grassland environments. An increase in bioproductivity at Spur Bog indicates a more mature terrestrial environment, i.e., the development of a peat bog at ~1610 cal BP (Figure 10e). Cooler and likely more arid conditions across Britain and north-western Europe during the ‘Maunder Minimum’ [65,66,83] lead to the expansion of grassland and the decline of woodland and wet heathland communities between ~1640 and 1720 cal AD, accompanied by increased local wildfire activity. During this time period, increased marine sediment accumulation and/or possibly fluctuating sea levels lead to the establishment of a mature dune system and the development of the ‘Little Sea Lagoon’ east of Spur Bog (Figure 10e,f).

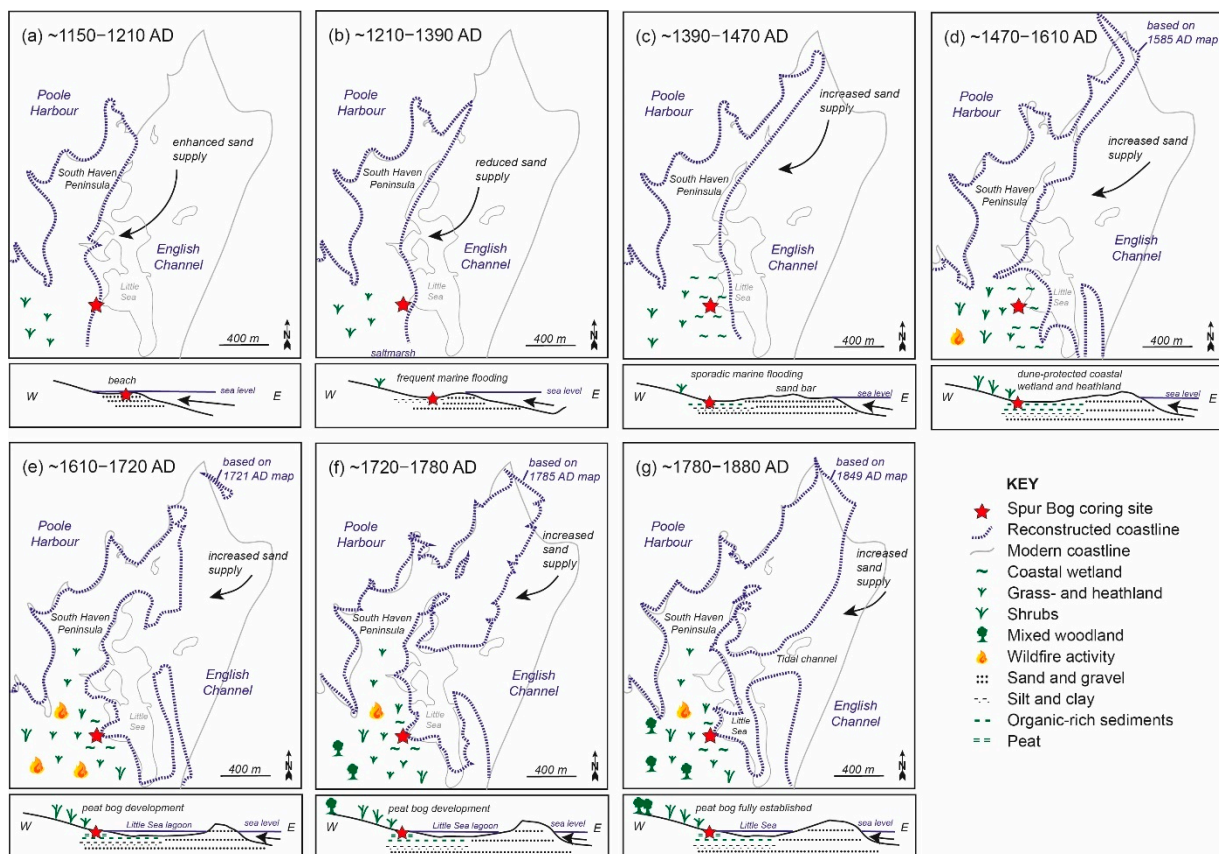


**Figure 10.** Schematic maps and cross-section models (not to scale) depicting geomorphological changes at the South Haven Peninsula and landscape/ecological changes at the site of Spur Bog (red star) during the last ~900 years. (a) The period ~1150–1210 AD: intertidal zone; (b) ~1210–1390 AD: coastal floodplain with saline tolerant grassland; (c) ~1390–1470 AD: sporadically flooded coastal wetland; (d) ~1470–1610 AD: dune-protected coastal wetland and heathland; coastline defined by using the map from [17]; (e) ~1610–1720 AD: spur peat bog development in an expanding grassland environment; increase in wildfire activity; coastline defined by using the map from [6,23]; (f) ~1720–1780 AD: spur peat bog development; transition from grassland to mixed woodland; development of Little Sea; decrease in wildfire activity; coastline defined by using the map from [6,25]; (g) ~1780–1880 AD: spur peat bog fully established; further development of Little Sea; further expansion of woodlands; coastline defined by using the map from [6,26].

Between 1720 AD and 1780 cal AD, vegetation at the Spur Bog transitioned from a grassland environment to a mixed woodland (Figure 10f), indicative of a climatic shift towards warmer and slightly wetter conditions, which is also supported by relatively low local wildfire activity. Throughout the late 18th and 19th centuries AD, woodlands in the southern periphery of the Spur Bog expanded further, as inferred from the continued increase in arboreal pollen and the decrease in herbaceous pollen concentrations. The significant increase in arboreal pollen values noted within the Spur Bog sequence are likely to reflect increased pollen transport from local woodland within the catchment area of the Little Sea (e.g., ‘Twelve Acre Wood’), which at that time developed from an open lagoon to a brackish lacustrine environment (Figure 10g). Stable aquatic pollen counts between ~1780 AD and 1880 cal AD in addition to the maintenance of high bioproductivity indicate the full establishment of the peat bog at Spur Bog and the recovery of wetland communities in this region as recorded in contemporaneous accounts [6,26]. Throughout much of the 19th century AD, low wildfire activity around the Spur Bog exhibit strong evidence of mild and relatively wet climatic conditions at the site, conforming to significantly increased precipitation and warmer temperatures noted across southern England and north-western Europe at that time [65,66,84].

According to historical records, environmental conditions at the Spur Bog continued to change throughout the 20th century AD, in response to the significant modification and intensification of human activities in the area, including the cessation of hunting and peat/furze cutting on heathlands in the Poole Basin by 1900 AD and 1918 AD, respectively [73], in addition to the construction of the Ferry Road adjacent to the Spur Bog in 1924 AD [6]. As such, by the 1930s, the Spur Bog and surrounding areas consisted of diverse mixed woodland, dry heathland and wet heathland habitats [6,85]. Land use of the South Haven Peninsula was altered dramatically once again during the Second World War when the area was used for military exercises, resulting in significant damage to Studland Beach, dune system and Little Sea—much of which is still evident in the present day [10,11]. Following the end of the Second World War, heathland habitats throughout the Poole Basin underwent grazing and were frequently burned, including a notable burning event in close proximity to the Spur Bog during the period 1959–1960 [73]. The Studland and Godlingston Heaths, containing the Spur Bog, were designated as a SSSI in 1954 [86]. Despite this, degradation of the heathland habitats in the area continued throughout the late 20th century AD due to poor management, anthropogenic pressures and climatic variability [57,67,87–89]. Following this, management of the Studland Heath was adapted to ensure the preservation and regeneration of heathland habitats, beginning in 1990 AD with the re-introduction of heathland flora and fauna, resulting in the expansion of stable heathland habitats on reclaimed Pine plantations within 14 years [89]. In addition, existing and regenerated areas of heathland are maintained through the periodic clearances and controlled burning [11], particularly to the benefit of dry heathland habitats, whilst a shift in climate towards warmer and wetter winters has facilitated the expansion of wet heathland/marshland since the 1930s [90,91]. These active management techniques have also been complemented by extensive ecological surveying of the Studland Heaths [90–93], against which the success of the aforementioned management strategies can be assessed.

## 5. Conclusions

The analysis of multi-proxy data extracted from the sedimentary sequence of the Spur Bog has enabled the reconstruction of environmental conditions in the area over the last ~900 years, significantly improving our understanding of the geomorphological formation, development and ecological conditions of the South Haven Peninsula during this time, which has previously relied upon sparse contemporary sources. Furthermore, the findings of this study demonstrate the sensitivity of the area to environmental changes associated with climate forcing and anthropogenic activity.

This study demonstrates that the Spur Bog sediments capture significant environmental variability, exhibiting a primary development phase (~1150–1470 cal AD) during which

marine processes were the dominant control upon environmental conditions at the site, facilitating the development of the South Haven Peninsula supporting coastal wetlands. This was followed by a secondary maturation phase (~1470–1900 cal AD) during which the Spur Bog sequence exhibits the formation of a lagoon bog, followed by a fully terrestrial peat bog and mixed woodland as the South Haven Peninsula continued to propagate eastward, whilst also responding to climatic instability and a range of anthropogenic pressures.

Therefore, the Spur Bog record significantly extends the previous palaeoenvironmental and geomorphological frameworks of the South Haven Peninsula, providing a record of environmental conditions between ~1150 cal AD and ~1900 cal AD in response to climatic and anthropogenic pressures. Thus, this record can serve as a valuable resource to enable the prediction and mitigation of future environmental changes at the Spur Bog amid an uncertain climate future.

**Supplementary Materials:** The following supporting information can be downloaded at: <https://www.mdpi.com/article/10.3390/quat5020027/s1>, Table S1: Spur Bog multi-proxy dataset.

**Author Contributions:** Conceptualisation, D.H. and S.W. (Sabine Wulf); methodology, D.H. and S.W. (Scarlett Wharram); validation, S.W. (Sabine Wulf) and M.H.; formal analysis, D.H. and S.W. (Scarlett Wharram); investigation, D.H., S.W. (Scarlett Wharram), H.B. and S.W. (Sabine Wulf); resources, M.H. and S.W. (Sabine Wulf); data curation, S.W. (Sabine Wulf) and M.H.; writing—original draft preparation, D.H.; writing—review and editing, S.W. (Sabine Wulf), M.H., S.W. (Scarlett Wharram) and H.B.; visualisation, D.H. and S.W. (Sabine Wulf); supervision, S.W. (Sabine Wulf) and M.H.; project administration, S.W. (Sabine Wulf); funding acquisition, S.W. (Sabine Wulf). All authors have read and agreed to the published version of the manuscript.

**Funding:** This research received no external funding.

**Institutional Review Board Statement:** Not applicable.

**Informed Consent Statement:** Not applicable.

**Data Availability Statement:** The data presented in this study are available in Supplementary Table S1.

**Acknowledgments:** We thank the National Trust and especially David Brown for their cooperation, including the granting of permission to carry out surveys within the Studland and Godlingston Heath and extraction of sediment cores from the Spur Bog.

**Conflicts of Interest:** The authors declare no conflict of interest.

## References

1. Harik, G.; Alameddine, I.; Maroun, R.; Rachid, G.; Bruschi, D.; Garcia, D.A.; El-Fadel, M. Implications of adopting a biodiversity-based vulnerability index versus a shoreline environmental sensitivity index on management and policy planning along coastal areas. *J. Environ. Manag.* **2017**, *187*, 187–200. [[CrossRef](#)] [[PubMed](#)]
2. Ward, N.D.; Megonigal, J.P.; Bond-Lamberty, B.; Bailey, V.L.; Butman, D.; Canuel, E.A.; Diefenderfer, H.; Ganju, N.K.; Goñi, M.A.; Graham, E.B.; et al. Representing the function and sensitivity of coastal interfaces in Earth system models. *Nat. Commun.* **2020**, *11*, 2458. [[CrossRef](#)] [[PubMed](#)]
3. IPCC. *Climate Change 2014: AR5 Synthesis Report. Contribution of Working Groups I, II and III to the Fifth Assessment Report of the Intergovernmental Panel on Climate Change*; Core Writing Team, Pachauri, R.K., Meyer, L.A., Eds.; IPCC: Geneva, Switzerland, 2014; 151p.
4. Nicholls, R.; Lowe, J.A. Benefits of mitigation of climate change for coastal areas. *Glob. Environ. Change* **2004**, *14*, 229–244. [[CrossRef](#)]
5. Martínez, M.; Intralawan, A.; Vázquez, G.; Pérez-Maqueo, O.; Sutton, P. The coasts of our world: Ecological, economic and social importance. *Ecol. Econ.* **2007**, *63*, 254–272. [[CrossRef](#)]
6. Diver, C. The physiography of South Haven Peninsula, Studland Heath, Dorset. *Geogr. J.* **1933**, *81*, 404–422. [[CrossRef](#)]
7. Gray, A.J. *Poole Harbour: Ecological Sensitivity Analysis of the Shoreline*; Institute of Terrestrial Ecology: Huntingdon, UK, 1985; 36p.
8. Long, A.J.; Scaife, R.G.; Edwards, R.J. Pine pollen in intertidal sediments from Poole Harbour, UK; implications for late-Holocene sediment accretion rates and sea-level rise. *Quat. Int.* **1999**, *55*, 3–16. [[CrossRef](#)]
9. Edwards, R.J. Mid-to late Holocene relative sea-level change in Poole Harbour, southern England. *J. Quat. Sci.* **2001**, *16*, 221–235. [[CrossRef](#)]
10. Cook, R.L. Spatial and Temporal Scales of the Morphodynamic Evolution within the Studland Complex. Ph.D. Thesis, Bournemouth University, Bournemouth, UK, 2007.

11. The National Trust. Coastal Management Policy in Purbeck. 2019. Available online: <https://nt.global.ssl.fastly.net/studland-bay/documents/coastal-management-policy-in-purbeck-february-2019.pdf> (accessed on 19 July 2021).
12. Bristow, C.R.; Freshney, E.C.; Penn, I.E. *Geology of the Country around Bournemouth*; Memoir of the Geological Survey of Great Britain; Sheet No. 329; HMSO: London, UK, 1991.
13. Gale, A. 1. The geology of Poole Harbour. In *The Ecology of Poole Harbour*; Humphreys, J., May, V., Eds.; Proceedings in Marine Science; Elsevier: Amsterdam, The Netherlands, 2005; Volume 7, pp. 9–23.
14. Studland and the South Haven Peninsula; Geology of the Wessex Coast of southern England—By Ian West. Available online: <http://www.southampton.ac.uk/~imw/Studland.html> (accessed on 10 August 2021).
15. Arkell, W.J. *The Geology of the Country around Weymouth, Swanage, Corfe and Lulworth*; Memoir of the Geological Survey; H.M. Stationery Office: Richmond, UK, 1947; 386p.
16. New Forest District Council. 2012 Update of Carter, D.; Bray, M.; Hooke, J. 2004. SCOPAC Sediment Transport Study. Available online: <http://scopac.org.uk/sts> (accessed on 25 April 2021).
17. Treswell, R. Survey of the Isle of Purbeck. 1586. Available online: <https://app.dorsetcouncil.gov.uk/bankes-archive/the-treswell-survey/> (accessed on 14 August 2021).
18. Camden, W. *Britannia Sive Florentissimorum Regnorum, Angliæ, Scotiæ, Hiberniæ, et Insularum Adiacentium ex Intima Antiquitate Chorographica Description*; George Bishop and John Norton: London, UK, 1607; pp. 181–182.
19. Lucas, P.J. William Camden, seventeenth-century atlases of the British Isles and the printing of Anglo-Saxon. *Antiqu. J.* **2018**, *98*, 219–244. [CrossRef]
20. Blaeu, J. *Comitatus Dorcestria, Sive Dorsettia: Vulgo Anglice Dorset Shire*; Amsterdam, The Netherlands. 1645. Available online: <https://collections.leventhalmap.org/search/commonwealth:ww72bp511> (accessed on 6 January 2022).
21. Saxton, C. *Christopher Saxton's 16th Century Maps*; Chatsworth Library: Los Angeles, CA, USA, 1992.
22. Keuning, J. *Blaeu's Atlas: Imago Mundi*; Taylor & Francis: Abingdon, UK, 1959; Volume 14, pp. 74–89.
23. Avery, J. An Actual Survey of the Coast from Arundel Haven in Sussex to St Aldans in Dorsetshire. 1721. Available online: <https://collections.rmg.co.uk/collections/objects/565476.html> (accessed on 7 June 2021).
24. Dummer, E.; Wiltshaw, T. South Coast of England Survey. 1698. Available online: <https://collections.rmg.co.uk/collections/objects/544971.html> (accessed on 10 June 2021).
25. MacKenzie, M. Survey of the South Coast of England. 1785. Available online: <https://www.dorsetlife.co.uk/2010/12/charting-poole-harbour/> (accessed on 25 July 2021).
26. Sheringham, R.N. MS Plan; Hydrographic Department, Admiralty. 1849. Available online: [https://assets.publishing.service.gov.uk/government/uploads/system/uploads/attachment\\_data/file/332228/UKHO-1849-Archives-Catalogue.pdf](https://assets.publishing.service.gov.uk/government/uploads/system/uploads/attachment_data/file/332228/UKHO-1849-Archives-Catalogue.pdf) (accessed on 12 July 2021).
27. Ordnance Survey. Dorset LI.SW. 1925. Available online: <https://maps.nls.uk/view/101447375> (accessed on 12 January 2022).
28. Lack, D.; Venables, L.S.V. The heathland birds of South Haven Peninsula, Studland Heath, Dorset. *J. Anim. Ecol.* **1937**, *6*, 62–72. [CrossRef]
29. Alvin, K.L. Observations on the lichen ecology of South Haven peninsula, Studland Heath, Dorset. *J. Ecol.* **1960**, *48*, 331–339. [CrossRef]
30. Liley, D.; Pickess, B.; Underhill-Day, J. *The Number and Distribution of Black-Necked Grebes and Other Water Birds at Studland, Dorset*; The Poole Harbour Study Group: Wareham, UK, 2006.
31. Carr, A.P. Experiments on Longshore Transport and Sorting on Pebbles: Chesil Beach, England. *J. Sediment. Petrol.* **1971**, *41*, 1084–1104.
32. Halcrow Group Limited. *Poole Bay and Harbour Coastal Strategy Study: Assessment of Flood and Coast Defense Options Poole Bay*; Halcrow Group Limited: Swindon, UK, 2004.
33. May, V. *Studland Beach: Changes in the Beach and Dunes and their Implications for Shoreline Management Between Poole Harbour and Old Harry*; Report to National Trust; Department of Conservation Sciences, Bournemouth University: Bournemouth, UK, 1977; 26p.
34. Long, A.J.; Tooley, M.J. Holocene sea-level and crustal movements in Hampshire and Southeast England, United Kingdom. *J. Coastal. Res.* **1995**, *17*, 299–310.
35. Shennan, I.; Horton, B. Holocene land-and sea-level changes in Great Britain. *J. Quat. Sci.* **2002**, *17*, 511–526. [CrossRef]
36. Moore, P.D.; Webb, J.A.; Collinson, M.E. *Pollen Analysis*; Blackwell Scientific Publications: Oxford, UK, 1991.
37. Faegri, K.; Kaland, P.E.; Krzywinski, K. *Textbook of Pollen Analysis*, 4th ed.; John Wiley & Sons Ltd.: Chichester, UK, 1989.
38. Juggins, S. Rioja: Analysis of Quaternary Science Data. 2020. Available online: <https://cran.r-project.org/package=rioja> (accessed on 14 January 2021).
39. Finsinger, W.; Kelly, R.; Fevre, J.; Magyari, E.K. A guide to screening charcoal peaks in macrocharcoal-area records for fire-episode reconstructions. *Holocene* **2014**, *24*, 1002–1008. [CrossRef]
40. Chambers, F.M.; Beilman, D.W.; Yu, Z. Methods for determining peat humification and for quantifying peat bulk density, organic matter and carbon content for palaeostudies of climate and peatland carbon dynamics. *Mires Peat* **2011**, *7*, 1–10.
41. Reimer, P.J.; Austin, W.E.N.; Bard, E.; Bayliss, A.; Blackwell, P.G.; Bronk Ramsey, C.; Butzin, M.; Cheng, H.; Edwards, R.L.; Friedrich, M.; et al. The IntCal20 Northern Hemisphere Radiocarbon Age Calibration Curve (0–55 cal kBP). *Radiocarbon* **2020**, *62*, 725–757. [CrossRef]
42. Bronk Ramsey, C. OxCal Version 4.4.2. 2020. Available online: <https://c14.arch.ox.ac.uk/oxcal.html> (accessed on 4 August 2021).

43. Brown, A.G.; Carpenter, R.G.; Walling, D.E. Monitoring Fluvial Pollen Transport, its Relationship to Catchment Vegetation and Implications for Palaeoenvironmental Studies. *Rev. Palaeobot. Palynol.* **2007**, *147*, 60–76. [[CrossRef](#)]
44. Tinner, W.; Conedera, M.; Gobet, E.; Hubschmid, P.; Wehrli, M.; Ammann, B. A palaeoecological attempt to classify fire sensitivity of trees in the southern Alps. *Holocene* **2000**, *10*, 565–574. [[CrossRef](#)]
45. Finsinger, W.; Tinner, W.; van der Knaap, W.O.; Ammann, B. The expansion of hazel (*Corylus avellana* L.) in the southern Alps: A key for understanding its early Holocene history in Europe? *Quat. Sci. Rev.* **2006**, *25*, 612–631. [[CrossRef](#)]
46. Gottschalk, M.K.E. *Storm Surges and River Floods in The Netherlands I (The Period 1400–1600)*; Van Gorcum: Assen, The Netherlands, 1975.
47. Lamb, H.H. *Climate, History and the Modern World*; Methuen: London, UK, 1982.
48. Lamb, H.H.; Frydendahl, K. *Historic Storms of the North Sea, British Isles and Northwest Europe*; Cambridge University Press: Cambridge, UK, 1991.
49. Wilcox, D.A.; Andrus, R.E. The role of *Sphagnum fimbriatum* in secondary succession in a road salt impacted bog. *Can. J. Bot.* **1987**, *65*, 2270–2275. [[CrossRef](#)]
50. Vasquez, E.A.; Glenn, E.P.; Guntenspergen, G.R.; Brown, J.J.; Nelson, S.G. Salt tolerance and osmotic adjustment of *Spartina alterniflora* (Poaceae) and the invasive *M* haplotype of *Phragmites australis* (Poaceae) along a salinity gradient. *Am. J. Bot.* **2006**, *93*, 1784–1790. [[CrossRef](#)] [[PubMed](#)]
51. Stofberg, S.F.; Klimkowska, A.; Paulissen, M.P.C.P.; Witte, J.P.M. *Potential Sensitivity of Fen Plant Species to Salinity*; Knowledge for Climate Programme Office: Utrecht, The Netherlands, 2014; Volume 113, 59p.
52. Lamb, H.H.; Brooks, C.E.P. *The English Climate*; English Universities Press: London, UK, 1964.
53. Brazell, J.H. *London Weather*; HMSO: London, UK, 1968.
54. Goosse, H.; Arzel, O.; Luterbacher, J.; Mann, M.E.; Renssen, H.; Riedwyl, N.; Timmermann, A.; Xoplaki, E.; Wanner, H. The origin of the European “Medieval Warm Period”. *Clim. Past* **2006**, *2*, 99–113. [[CrossRef](#)]
55. Chambers, F. The ‘Little Ice Age’: The first virtual issue of The Holocene. *Holocene* **2016**, *26*, 335–337. [[CrossRef](#)]
56. Ilyashuk, E.A.; Heiri, O.; Ilyashuk, B.P.; Koinig, K.A.; Psenner, R. The Little Ice Age signature in a 700-year high-resolution chironomid record of summer temperatures in the Central Eastern Alps. *Clim. Dyn.* **2019**, *52*, 6953–6967. [[CrossRef](#)] [[PubMed](#)]
57. Webb, N.R.; Haskins, L.E. An ecological survey of heathlands in the Poole Basin, Dorset, England, in 1978. *Biol. Conserv.* **1980**, *17*, 281–296. [[CrossRef](#)]
58. Rumsby, B.T.; Macklin, M.G. *River Response to the Last Neoglacial (The ‘Little Ice Age’) in Northern, Western and Central Europe*; Geological Society, Special Publications: London, UK, 1996; Volume 115, pp. 217–233.
59. Mörner, N.A. Solar Minima, Earth’s rotation and Little Ice Ages in the past and in the future: The North Atlantic-European case. *Glob. Planet. Change* **2010**, *72*, 282–293. [[CrossRef](#)]
60. Macadam, J. English Weather: The Seventeenth-Century Diary of Ralph Josselin. *J. Interdiscip. Hist.* **2012**, *43*, 221–246. [[CrossRef](#)]
61. Alheit, J.; Hagen, E. Long-term climate forcing of European herring and sardine populations. *Fish. Oceanogr.* **1997**, *6*, 130–139. [[CrossRef](#)]
62. Reid, G.C. Solar forcing of global climate change since the mid-17th century. *Clim. Change* **1997**, *37*, 391–405. [[CrossRef](#)]
63. Parker, G. *Global Crisis: War, Climate Change, & Catastrophe in the Seventeenth Century*; Yale University Press: New Haven, CT, USA, 2013.
64. González-Hidalgo, J.C.; Peña-Angulo, D.; Beguería, S. Temporal variations of trends in the Central England temperature series. *Cuad. Investig. Geográfica* **2020**, *46*, 345–369. [[CrossRef](#)]
65. Barbour-Mercer, S.A. Prosecution and Process: Crime and Criminal Law in Late Seventeenth-Century Yorkshire. Ph.D. Thesis, University of York, York, UK, 1988.
66. Waddell, B. Governing England through the manor courts, 1550–1850. *Hist. J.* **2012**, *55*, 279–315. [[CrossRef](#)]
67. Natural England. Dorset’s Purple Patch: Dorset Heathlands from Pre-History to the Present Day. 2015. Available online: <https://www.poole.gov.uk> (accessed on 10 January 2022).
68. McGrath, M.J.; Luyssaert, S.; Meyfroidt, P.; Kaplan, J.O.; Bürgi, M.; Chen, Y.; Erb, K.; Gimmi, U.; McInerney, D.; Naudts, K.; et al. Reconstructing European forest management from 1600 to 2010. *Biogeosciences* **2015**, *12*, 4291–4316. [[CrossRef](#)]
69. Parker, D.E.; Legg, T.P.; Folland, C.K. A new daily Central England Temperature Series, 1772–1991. *Int. J. Climatol.* **1992**, *12*, 317–342. [[CrossRef](#)]
70. Alexander, L.V.; Jones, P.D. Updated precipitation series for the UK and discussion of recent extremes. *Atmos. Sci. Lett.* **2001**, *1*, 142–150. [[CrossRef](#)]
71. Stagg, D.J. *A Calendar of New Forest Documents: The Fifteenth to the Seventeenth Centuries*; Hampshire Record Office for Hampshire County Council: Winchester, UK, 1983.
72. Tavener, L.E. *Dorset. Part 88 in The Land of Britain*; The Report of the Land Utilization Survey of Britain; Dudley Stamp: London, UK, 1940.
73. Moore, N.W. The heaths of Dorset and their conservation. *J. Ecol.* **1962**, *50*, 369–391. [[CrossRef](#)]
74. Wigley, T.M.L.; Lough, J.M.; Jones, P.D. Spatial patterns of precipitation in England and Wales and a revised, homogeneous England and Wales precipitation series. *J. Climatol.* **1984**, *4*, 1–25. [[CrossRef](#)]
75. Dürschmied, E. *The Weather Factor*; Hodder & Stoughton: London, UK, 2000.
76. Grove, J.M. *The Little Ice Age*; Routledge: London, UK, 2012.

77. Fagan, B. *The Little Ice Age: How Climate Made History 1300–1850*; Hachette: New York, NY, USA, 2019.
78. Brooks, C.E.P. *Climate in Everyday Life*; Ernest Benn: London, UK, 1950.
79. Legg, R. *Brownsea: Dorset's Fantasy Island*; The Dorset Publishing Company: Sherborne, UK, 1986; 80p.
80. Garnett, O. *Brownsea Castle*; The National Trust: Swindon, UK, 2005.
81. Wilson, K. The Time Factor in the Development of Dune Soils at South Haven Peninsula, Dorset. *J. Ecol.* **1960**, *48*, 341–359. [[CrossRef](#)]
82. Lane, F.W. The Elements Rage. Newton Abbot: David and Charles. *Q. J. R. Meteorol. Soc.* **1966**, *93*, 280.
83. Owens, M.J.; Lockwood, M.; Hawkins, E.; Usoskin, I.; Jones, G.S.; Barnard, L.; Schurer, A.; Fasullo, J. The Maunder minimum and the Little Ice Age: An update from recent reconstructions and climate simulations. *J. Space Weather Space Clim.* **2017**, *7*, A33. [[CrossRef](#)]
84. Zumbühl, H.J.; Steiner, D.; Nussbaumer, S.U. 19th century glacier representations and fluctuations in the central and western European Alps: An interdisciplinary approach. *Glob. Planet. Change* **2008**, *60*, 42–57. [[CrossRef](#)]
85. Good, R. *A Geographical Handbook of the Dorset Flora*; The Dorset Natural History and Archaeological Society, County Museum: Dorchester, UK, 1948; 255p.
86. Mahdi, H. Preservation Plan for Studland and Godlingston heaths in Dorset. Ph.D. Thesis, Newcastle University, Newcastle, UK, 2015.
87. Webb, N.R. Changes on the heathlands of Dorset, England between 1978 and 1987. *Biol. Conserv.* **1990**, *51*, 272–286. [[CrossRef](#)]
88. Rose, R.J.; Webb, N.R.; Clarke, R.T.; Traynor, C.H. Changes on the heathlands in Dorset, England, between 1987 and 1996. *Biol. Conserv.* **2000**, *93*, 117–125. [[CrossRef](#)]
89. Forup, M.L.; Henson, K.S.; Craze, P.G.; Memmott, J. The restoration of ecological interactions: Plant-pollinator networks on ancient and restored heathlands. *J. Appl. Ecol.* **2008**, *45*, 742–752. [[CrossRef](#)]
90. Carroll, T.; Gillingham, P.K.; Stafford, R.; Bullock, J.M.; Diaz, A. Improving estimates of environmental change using multilevel regression models of Ellenberg indicator values. *Ecol. Evol.* **2018**, *8*, 9739–9750. [[CrossRef](#)] [[PubMed](#)]
91. Carroll, T. Unravelling Abiotic and Biotic Drivers of Biodiversity Change in Local Plant and Invertebrate Communities after 80 Years—a Re-Visitation Study on the Studland Peninsula. Ph.D. Thesis, Bournemouth University, Bournemouth, UK, 2020.
92. Kragh, G. The motivations of volunteers in citizen science. *Environ. Sci.* **2016**, *25*, 32–35.
93. Munns, L.H. Is It All about the Ants? What Are the Factors Influencing the Presence of *Plebejus Argus* (The Silver-Studded Blue Butterfly) On Studland Peninsula? Ph.D. Thesis, Bournemouth University, Bournemouth, UK, 2017.